An Overview of Finite Difference Modeling of Hydrodynamic Systems

Donald C. Raney
The University of Alabama

MASGP-83-028

Mississippi-Alabama Sea Grant Consortium

Project Number: R/EN-1

Program Year: 1983

Grant Number: NA81AA-D-00050

This publication was supported by the National Sea Grant College Program of the U.S. Department of Commerce's National Oceanic and Atmospheric Administration under NOAA Grant # NA81AA-D-00050, the Mississippi-Alabama Sea Grant Consortium and The University of Alabama. The views expressed herein do not necessarily reflect the views of any of those organizations.

AN OVERVIEW OF FINITE DIFFERENCE MODELING OF HYDRODYNAMIC SYSTEMS

by

Donald C. Raney
Professor of Engineering Mechanics
The University of Alabama
Tuscaloosa, Alabama

Presented at Short Course
"Numerical Modeling for Engineers"
at
U.S. Army Waterways
Experiment Station
Vicksburg, Mississippi
March 14-18, 1983

Introduction

Numerical modeling is a rapidly developing discipline which can be attributed in part to the general availability of fast, large memory digital computers. A fast, large memory computer is generally necessary to obtain the desired resolution from the model results in a reasonable amount of computer time. Prior to the 1970's access to large, fast computers was restricted to the larger government or university research laboratories; however, this type computer is now generally available at most universities. As a consequence, development and use of state-of-the-art numerical models are now common within the academic community.

A numerical model basically consists of a numerical algorithm which has been developed from the differential equations governing the physical phenomena. Several methods exist for developing the numerical algorithm, falling generally into two types of formulation; finite difference and finite element. Finite element techniques are used extensively in solid mechanics but to a much smaller extent in fluid mechanics. For a variety of reasons finite difference techniques have gained greater acceptance in hydrodynamic modeling and will be used exclusively in this treatment of numerical modeling of hydrodynamic systems. Hydrodynamic systems is a general term intended to denote a body of water with a free surface such as an estuary, lake or river. A one-dimensional, two-dimensional or three-dimensional model formulation may be required depending on the individual problem to be considered.

Numerical fluid mechanics is a separate discipline, with many features distinct from experimental fluid mechanics and theoretical fluid mechanics. The numerical modeler, however, does have many problems in common with the physical modeler. The numerical modeler (as does the physical modeler) must interface with individuals involved in the collection of prototype data to provide information for "verification" of the numerical model. Any model must be verified by demonstrating that the model can produce results which agree with measured values for some set of boundary conditions before much credibility can be associated with the model results. There are a wide range of numerical models; however, certain features and concepts are common to most models. An understanding of some fundamental concepts will yield benefits in a wide range of model applications.

Some of the material presented in these notes has been adapted from material found in publications by Roache[1], Abbott[2] and Basco[3]. The reader interested in more detailed information about numerical modelling or computational fluid mechanics should consult these references.

Introduction to Basic Finite Difference Concepts

Consider the flow in a stream or river. It is desired to collect surface velocity data at six (6) equi-spaced locations across the stream (in the x direction). The velocities which were measured at time t_0 are shown plotted as vectors in Figure 1. Assume that it is desired to evaluate the rate of change of velocity (i.e., the velocity gradient) in the x direction at point 3 for this set of data. In mathematical terms, it is desired to evaluate (dV/dX_3), where the subscript 3 indicates the location at which the derivative is to be evaluated.

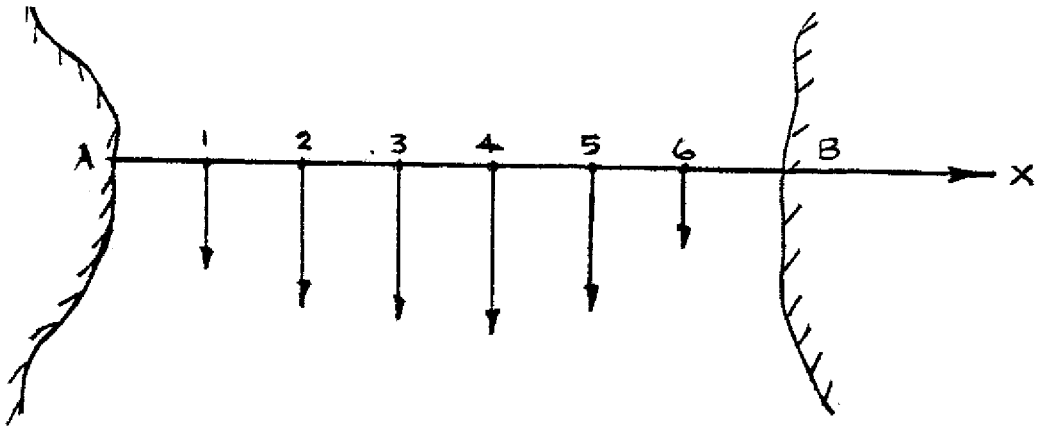

Figure 1. Velocity Distribution Across a Stream

One method to evaluate $(dV/dX)_3$ involves graphically constructing a smooth curve through the measured data points and then constructing a tangent to this curve at point 3. This is illustrated in Figure 2. This method involves graphical or numerical curve fitting techniques in addition to the original measured velocity data.

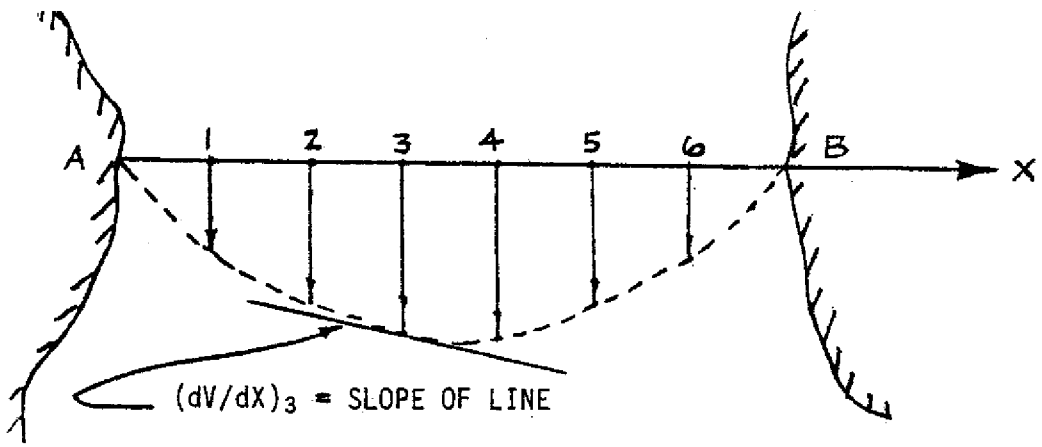

Figure 2. Graphical Evaluation of the Velocity Gradient

A second general method for evaluation $(dV/dX)_3$ uses only the measured velocity data. In this case the derivative can be represented in terms of various combinations of the velocity at point 3 and/or neighboring velocity values. Three possible derivative formulations are intuitively apparent. These are the forward difference, the backward difference and the central difference representation. These derivative formulations are indicated in Figures 3, 4, and 5. The forward difference evaluation uses the velocity values at point 3 and point 4 (the point spatially forward of point 3) to evaluate the derivative. The backward difference uses the velocity values at point 3 and point 2 (the point spatially behind point 3) to evaluate the

derivative. The central difference uses the velocity values at points 2 and 4 (the points on each side of point 3) to evaluate the derivative. If the change in velocity in the x direction is gradual, as in this example, the various formulations for the derivative will yield very similar numerical values. On the other hand, if the velocity changes rapidly in the x direction, the various derivative formulations can yield significantly different results as illustrated in Figure 6. The physical problem may in some cases dictate which derivative formulation should be used. For example, to evaluate (dV/dX) at the boundary of the stream (point A) it would appear necessary to use a forward difference. For many cases, however, the actual derivative formulation used in the model is based upon less apparent factors.

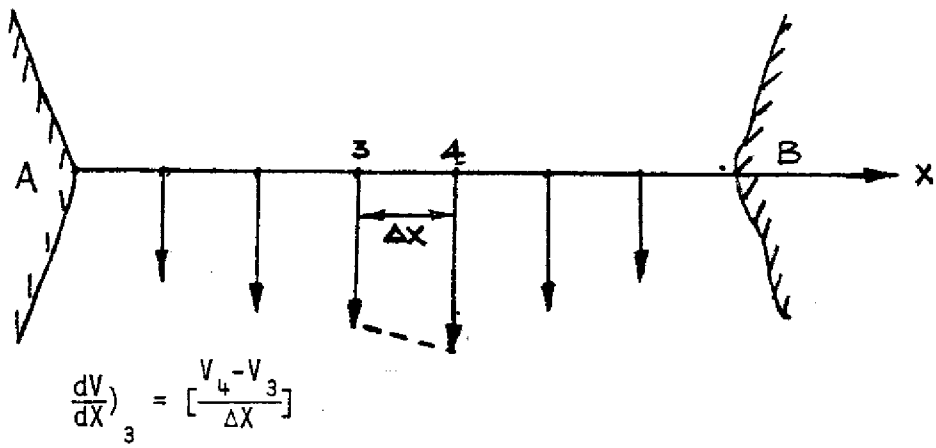

Figure 3. Forward Difference Representation of a Derivative

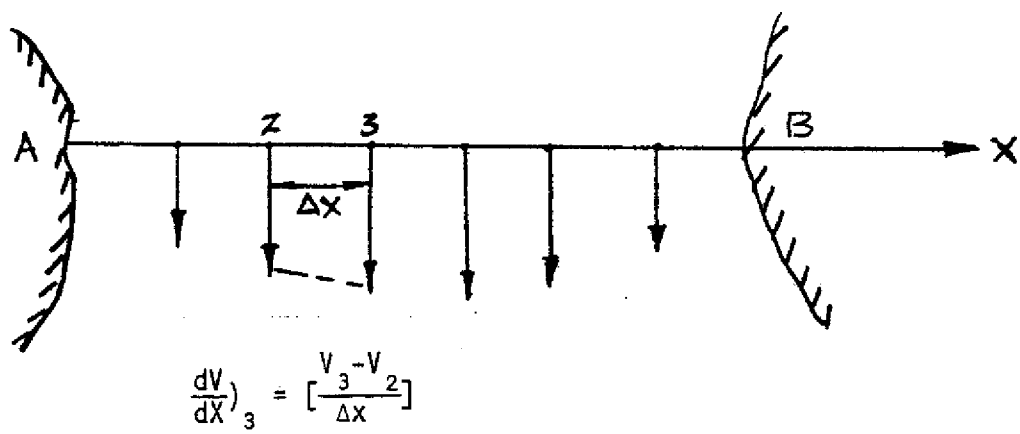

Figure 4. Backward Difference Representation of a Derivative

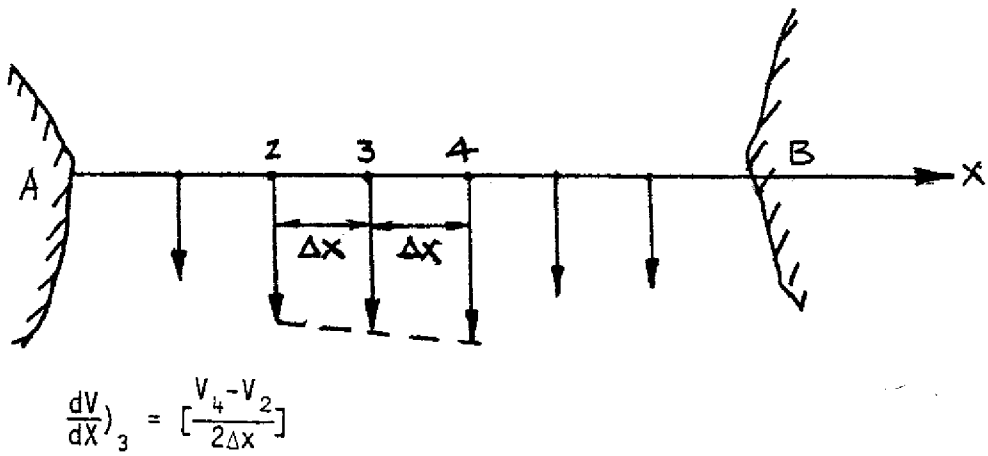

Figure 5. Central Difference Representation of a Derivative

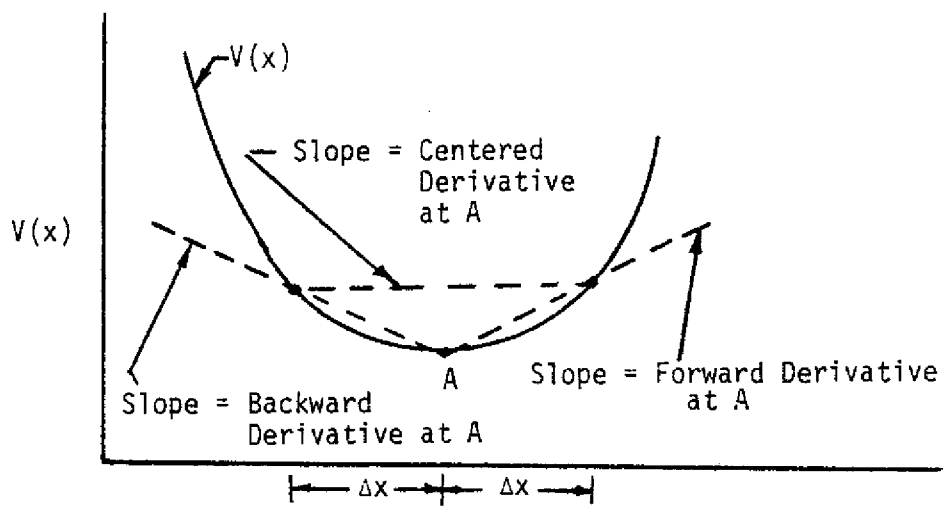

Figure 6. Different Representations of Derivative at a Point

The finite difference formulation is deceptively simple. The several formulations which have been presented were intuitive. This approach to formulating the derivatives, however, provides no indication of their associated errors of approximation. Other more formal methods are available for obtaining approximations to derivatives and their associated errors of approximation. The best approach is to use a Taylor series expansion about the point of interest. The Taylor series expansion assumes that the quantity to be represented is continuous in the region of interest as shown in Figure 7. Furthermore, if the value of the function and the derivatives of the function are known at some point, the value of the function at a neighboring point is given by:

$$V_{j+1} = V_j + \left(\frac{dV}{dX}\right)_j \Delta X + \left(\frac{d^2V}{dX^2}\right)_j \frac{\Delta X^2}{2!} + \left(\frac{d^3V}{dX^3}\right)_j \frac{\Delta X^3}{3!} + \text{---H.O.T.} \qquad (1)$$

The subscripts refer to space location and H.O.T. means all the remaining higher order terms (i.e., terms of smaller magnitude).

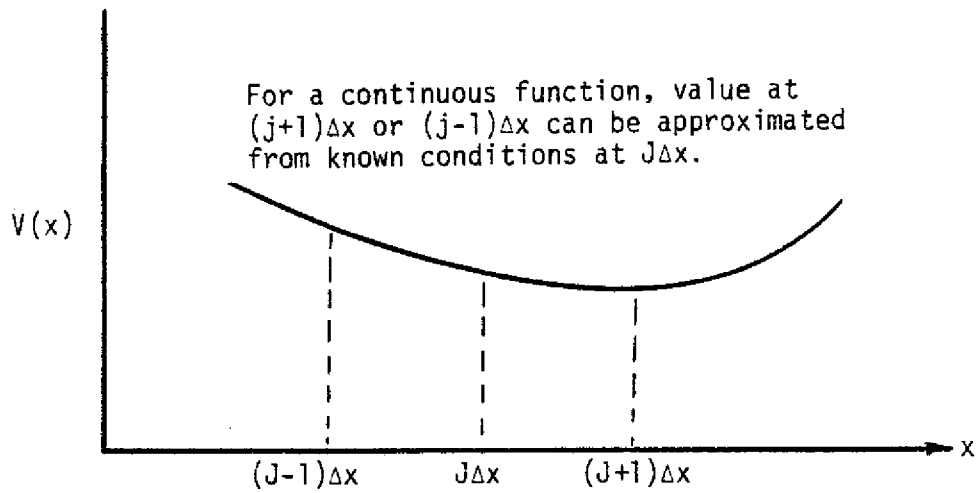

Figure 7. Taylor Series Expansion for a Continuous Variable

Solving for the first derivative:

$$\left(\frac{dV}{dX}\right)_j = \left(\frac{V_{j+1}-V_j}{\Delta X}\right) - \left(\frac{d^2V}{dX^2}\right)_j \frac{\Delta X}{2!} - \left(\frac{d^3V}{dX^3}\right)_j \frac{\Delta x^2}{3!} - \text{H.O.T.}$$

If the Taylor series expansion is truncated to include only the first term

$$\left(\frac{dV}{dX}\right)_j = \left[\frac{V_{j+1}-V_j}{\Delta X}\right] \qquad (2)$$

then the remaining terms are the "truncation errors" and this remainder approaches zero proportionally as Δx, approaches zero. Thus the error of the approximation is of order Δx, simply written $O(\Delta x)$. Equation (2) is the lowest accuracy or "first" order, forward difference approximation to a first derivative. Equation (2) was previously indicated as a forward, finite-difference "formula", but use of the formal Taylor series gives additional information on accuracy.

Similarly, the backward difference approximation of $(dV/dX)_j$ from j to j-1 over a negative distance ($-\Delta x$) will give

$$\left(\frac{dV}{dX}\right)_j = \frac{V_j-V_{j-1}}{\Delta X} + \left(\frac{d^2V}{dX^2}\right)_j \frac{\Delta X}{2!} - \left(\frac{d^3V}{dX^3}\right) \frac{\Delta X^2}{3!} + \text{H.O.T.} \qquad (3)$$

with the truncation error again of $O(\Delta x)$. To obtain a centered or central difference approximation for $(dV/dX)_j$, again apply the Taylor series from j to j+1 and from j to j-1. This is equivalent to adding Equations (1) and (3) to yield

$$2\left(\frac{dV}{dX}\right)_j = \frac{V_{j+1}-V_j}{\Delta X} + \frac{V_j-V_{j-1}}{\Delta X} - \left(\frac{d^2V}{dX^2}\right)_j \frac{\Delta X}{2!} + \left(\frac{d^2V}{dX^2}\right)_j \frac{\Delta X}{2!} - 2\left(\frac{d^3V}{dX^3}\right)_j \frac{\Delta X^2}{3!}$$

$$- \left(\frac{d^4V}{dX^4}\right)_j \frac{\Delta X^3}{4!} + \left(\frac{d^4V}{dX^4}\right)_j \frac{\Delta X^3}{3!} - 2\left(\frac{d^5V}{dX^5}\right)_j \frac{\Delta X^4}{5!} + H.O.T.$$

Dividing thru by 2 and cancelling like terms gives

$$\left(\frac{dV}{dX}\right)_j = \left[\frac{V_{J+1}-V_{J-1}}{2\Delta X}\right] - \left(\frac{d^3V}{dX^3}\right)_j \frac{\Delta X^2}{3!} - \left(\frac{d^5V}{dX^5}\right)_j \frac{\Delta X^4}{5!} + H.O.T. \qquad (4)$$

so that the truncation error is now of $O(\Delta x^2)$ meaning the remainder will go to zero faster as Δx approaches zero. Thus the centered finite difference is of higher order accuracy or second order accurate in this case.

Summarizing, the basic ways to approximate first derivatives in space are:

1. Forward-difference $O[\Delta x]$
$$\left(\frac{dV}{dX}\right)_j = \left[\frac{V_{j+1}-V_j}{\Delta X}\right] \qquad (5)$$

2. Backward-difference $O[\Delta x]$
$$\left(\frac{dV}{dX}\right)_j = \left[\frac{V_j-V_{j-1}}{\Delta X}\right] \qquad (6)$$

3. Centered-difference $O[\Delta x^2]$
$$\left(\frac{dV}{dX}\right)_j = \left[\frac{V_{j+1}-V_{j-1}}{2\Delta X}\right] \qquad (7)$$

In general, centered differences are more accurate as indicated by the Taylor Series expansion.

For most applications the numerical accuracy of first-order approximations is sufficient. Occasionally, the need arises to consider use of higher-order approximation formulas for improved accuracy. These formulas can be derived by writing additional, higher-order derivatives appearing in the truncation error as a finite-difference.

For example, in (1) the first truncation error term contains $(d^2V/dx^2)_j$ which could be approximated as a first order, forward difference about "point j" as follows. Repeating (1) here as

$$V_{j+1} = V_j + \left(\frac{dV}{dX}\right)_j \Delta X + \left(\frac{d^2V}{dX^2}\right)_j \frac{\Delta X^2}{2!} + \left(\frac{d^3V}{dX^3}\right)_i \frac{\Delta X^3}{3!} + H.O.T. \qquad (1)$$

and now expanding between j and j+2 gives

$$V_{j+2} = V_j + 2\left(\frac{dV}{dX}\right)_j \Delta X + 4\left(\frac{d^2V}{dX^2}\right)_j \frac{\Delta X^2}{2!} + 8\left(\frac{d^3V}{dX^3}\right)_j \frac{\Delta X^3}{3!} + H.O.T. \quad (8)$$

Multiply (1) by 2 and subtract (1) from (8) to obtain

$$\left(\frac{d^2V}{dX^2}\right)_j = \left[\frac{V_{j+2}-2V_{j+1}-V_j}{\Delta X^2}\right] - \left(\frac{d^3V}{dX^3}\right) \Delta X + H.O.T. \quad (9)$$

Note that this second derivative is only of $O(\Delta x)$ accuracy. Putting (9) into (2) gives

$$\left(\frac{dV}{dX}\right)_j = \left[\frac{V_{j+1}-V_j}{\Delta X}\right] - \left[\frac{V_{j+2}-2V_{j+1}+V_j}{\Delta X^2}\right] \frac{\Delta X}{2} + \left[-\frac{\Delta X^2}{3!} + \frac{\Delta X^2}{2!}\right]\left(\frac{d^2V}{dX^2}\right)_j + H.O.T. \quad (10)$$

or

$$\left(\frac{dV}{dX}\right)_j = \left[\frac{-V_{j+2}+4V_{j+1}-3V_j}{2\Delta X}\right] + O(\Delta X^2) \quad (11)$$

Thus the first derivative (forward difference) is made of higher order accuracy ($O(\Delta x^2)$) by using more than two grid points in the finite difference algorithm.

In a similar manner the higher truncation error terms can be approximated by finite-differences and combined with the original expression to obtain formulas involving even more grid points. This work has been performed by many numerical analysts and can be found documented in the literature.

Model Partial Differential Equations

Most physical processes are described by partial differential equations derived from physical laws. The partial differential equations are typically of a form not amenable to analytical solutions. Numerical methods such as the finite difference method are used to obtain approximate solutions to the governing partial differential equations. The simplest such partial differential equation in fluid mechanics is the scalar wave equation. The dependent variable of interest is water depth (h) which varies in time (t) and in one spatial direction (x). The partial differential equation that arises can be written:

$$\frac{\partial h}{\partial t} + C \frac{\partial h}{\partial x} = 0 \quad (12)$$

where C is a real constant.

This equation comes from the kinematic description of a flood moving (flood routing) down a river as derived from the conservation of mass. In

symbols, this statement that inflow minus outflow equals storage becomes:

$$\frac{\partial Q}{\partial X} + b_s \frac{\partial h}{\partial t} = 0 \qquad (13)$$

where:

Q = volumetric flowrate,

b_s = the storage width, and

h = the water depth.

Using the functional relationship between h and Q (stage-discharge) equation (13) can be transformed into an equation where h is the only dependent variable; i.e.,

$$\frac{\partial h}{\partial x} + C(h) \frac{\partial h}{\partial x} = 0$$

In this equation C(h) is essentially a celerity for propagation of differential disturbances in the surface elevation. Furthermore, taking C(h)=C as locally constant essentially "linearizes" the equation to simplify the discussion.

$$\frac{\partial h}{\partial t} + C \frac{\partial h}{\partial x} = 0 \qquad C = \text{real, constant} \qquad (15)$$

Equation (15) can be called the pure advection equation for it describes how the dependent variable, h is advected (moved) in one space dimension and time by a constant velocity; i.e., the celerity, C. As such, it is a model equation for many physical processes in science and engineering including: density variations of a gas propagating in a tube; a stream of automobile traffic in heavy traffic flow; flow of a glacier; the conservation of a group of waves of local wave number (k) moving with the group celerity; the advection of a substance (pollutants) in air or water; and many others. The "hydraulic", water depth meaning for h will be retained in these discussions. This equation was the basis for many early attempts at flood routing calculation for rivers but has been replaced in recent years by the complete, dynamic equations of motion plus continuity.

Physically, if successive "pictures" are taken of the river-level profile and the water surface is plotted at various times, a three-dimensional "model" results as shown in Figure 8. The variation of h with x and t appears as a "solution surface" which by definition means that the continuum, partial differential equation (along with appropriate boundary conditions) is satisfied at all "points" on this solution surface. A continuous solution surface in time and space is obtained as a solution of the partial differential equation. Generally speaking, all the infinite number of points on the solution surface are not of interest but only a small discrete number of the most interesting ones. Consequently, it is a logical extension to strive for "solutions" at only a discrete number of points in the solution field. The approximation of derivatives by discrete numbers of local points to form finite-differences

and the algebraic solution of the resulting equations representing PDE's for various initial and/or boundary conditions is called the Finite-Difference Method (FDM). The concept of discretization where a continuous domain is represented by a discrete number of grid points or adjacent grid areas is fundamental to all numerical methods.

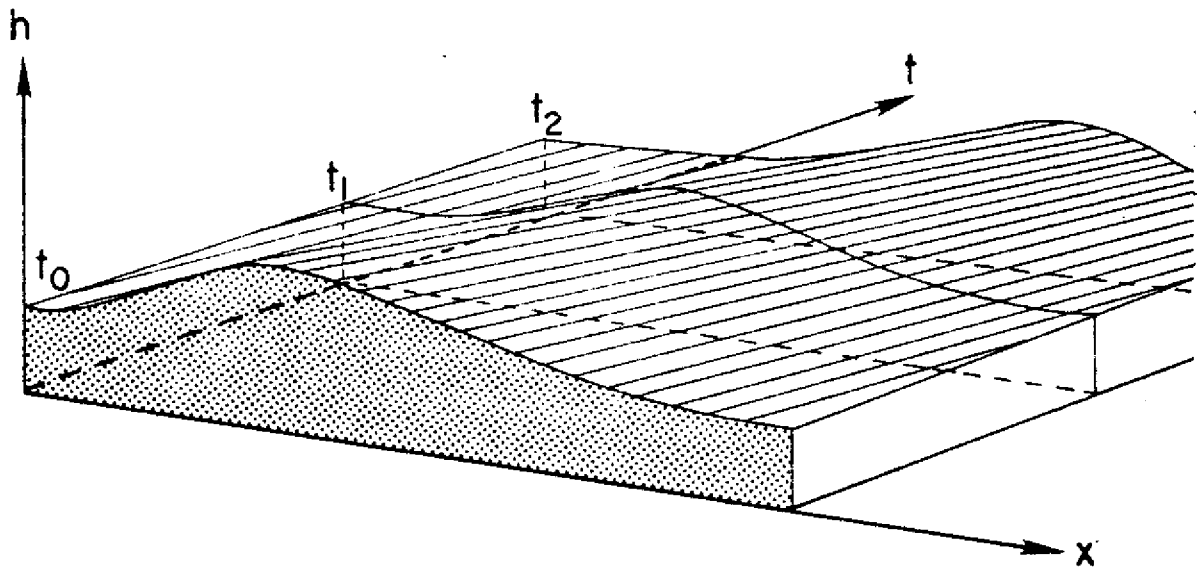

Figure 8. River Profile at Successive Times-Solution Surface

Finite-Difference Approximations

The concepts of a differential equation with solution known about infinitesimal regions and for all points can be extended to a finite-sized region and fixed number of points. A small patch of solution surface shown in Figure 8 has been expanded in Figure 9a and a finite grid drawn upon the solution surface. A projection of this grid on the x-t plane is also shown in Figure 9a and schematized in Figure 9b. The grid points are separated by distances Δx and Δt which are taken here as constants. The location of each grid point (j,n) is then established. The use of indices j, j+1, j-1, etc. for the x-direction space points and n, n+1, n-1, etc. for the time interval "points" has become somewhat standard.

Figure 10a shows a section of the solution surface along the x-axis at some time level, n Δt so that the slope of this line at any point, A, is $\partial h/\partial x$. Figure 10b is the analogous t-axis section and shows gradient $\partial h/\partial t$.

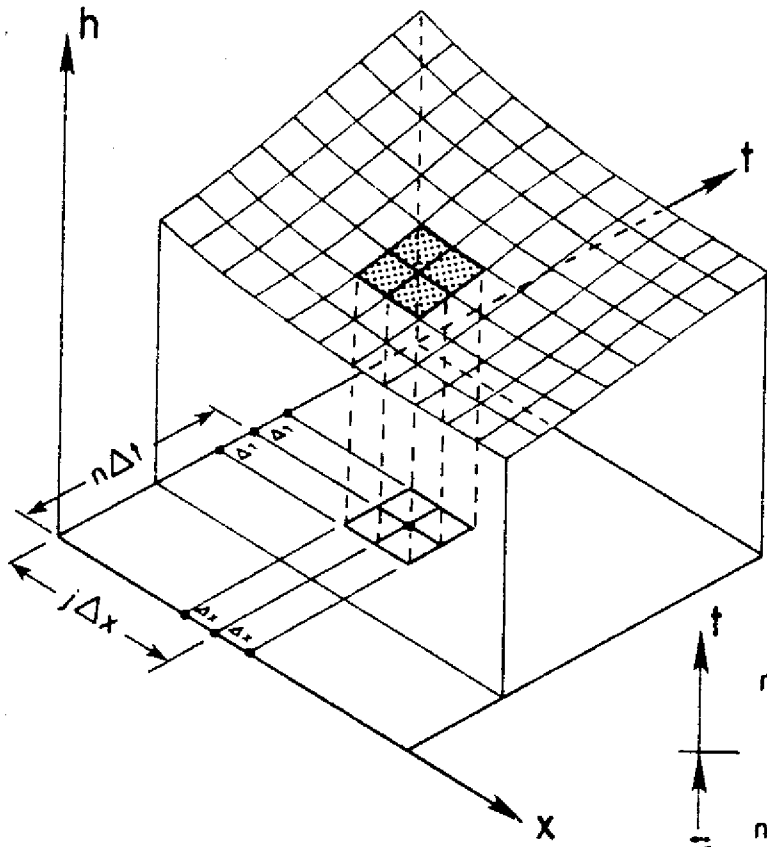

Figure 9a. Small Patch of Solution Surface with Grid

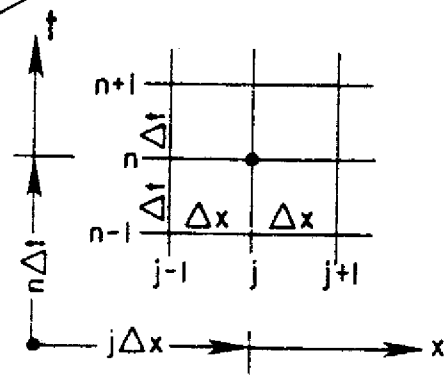

Figure 9b. Grid on x-t Plane

Using finite difference techniques, the various derivatives in the differential equations are approximated numerically in terms of distinct values of the variables at the cells. The differential equations are thus replaced by a numerical algorithm which can be solved numerically for values of the surface elevation for each cell in the system. As observed in the earlier representation of (dV/dX), the derivative representations are not unique. The finite difference representation of the governing differential equations can therefore be represented in several forms. Choosing the most appropriate representation for a particular differential equation involves the "art" of numerical modeling as opposed to the science of numerical modeling. Some of the difficulties in numerical modeling arise because some very logical finite difference representations do not work and some apparently minor changes in the finite difference equations can produce significantly different results.

Explicit and Implicit Representation of a Differential Equation

Consider the linearized wave equation

$$\frac{\partial h}{\partial t} + C \frac{\partial h}{\partial x} = 0 \qquad (12)$$

There is only one spatial variable (x) involved along with the variation in time (t). To completely define the problem an appropriate set of boundary conditions must be defined. A schematic representation is shown in Figure 11 for a one-dimensional system of finite difference cells.

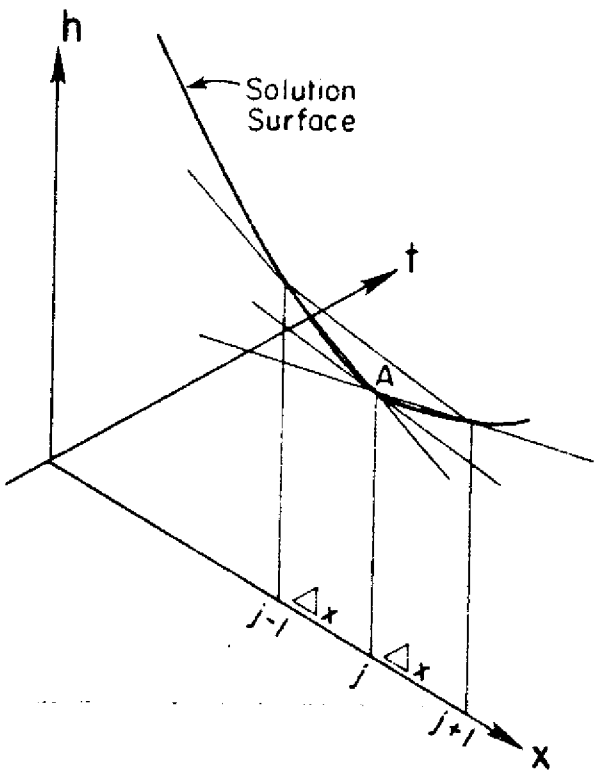

Figure 10a. Solution Surface Along x-axis for Any Time t

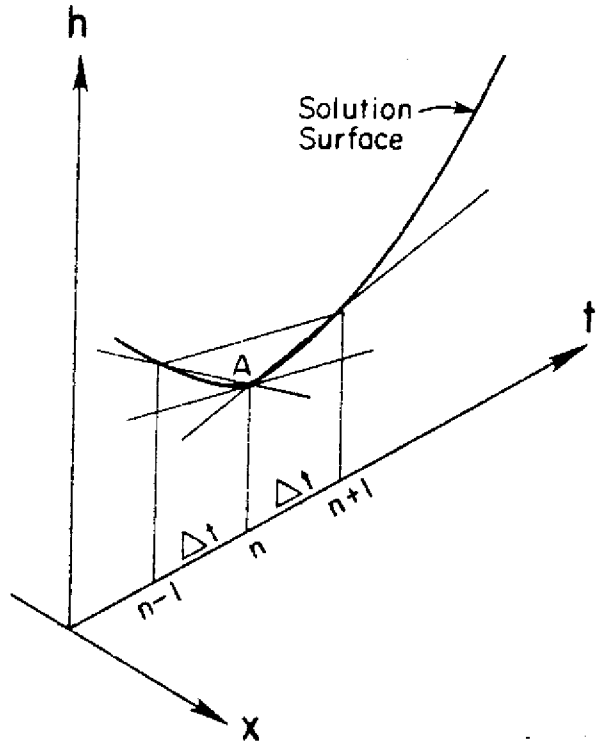

Figure 10b. Solution Surface Along t-axis for Any Time x

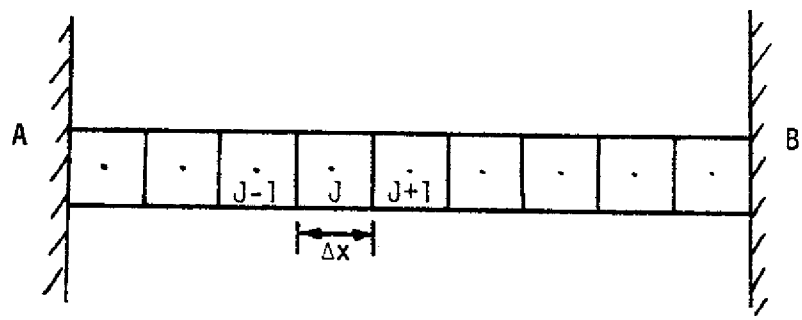

Figure 11. One-Dimensional Finite Difference Grid

Assume that the values of h are known at time level n for all of the finite difference grid and it is desired by finite difference techniques to calculate the values for h at some later time (level n+1). How is the finite difference equation formulated? To illustrate the method, consider the appropriate finite difference expressions for cell j of the grid drawn in Figure 11.

There are several possibilities for formulation of the various derivatives. In denoting values of the individual cell variables, superscripts and subscripts are used. The superscript indicates the position in time while the subscripts denote the spatial location. Thus h_j^n indicates the value of h for cell j at time level n. Some possible formulations of the derivatives are as follows:

$$\left(\frac{\partial h}{\partial t}\right)_j^n = \left[\frac{h_j^{n+1} - h_j^n}{\Delta t}\right] \qquad \text{(forward difference in time)}$$

$$\left(\frac{\partial h}{\partial t}\right)_j^n = \left[\frac{h_j^{n+1} - h_j^{n-1}}{2\Delta t}\right] \qquad \text{(centered difference in time)}$$

Note that if a centered time difference is used, the velocity values at time level n-1 are introduced. Thus, the value of h at point j for n-1 is used rather than the values at n to calculate the values of h at n+1 if the centered time difference is used.

$$\left(\frac{\partial h}{\partial x}\right)_j^n = \left[\frac{h_{j+1}^n - h_j^n}{\Delta X}\right] \qquad \text{(forward spatial difference using at n)}$$

$$\left(\frac{\partial h}{\partial x}\right)_j^n = \left[\frac{h_j^n - h_{j-1}^n}{\Delta X}\right] \qquad \text{(backward spatial difference using values at n)}$$

$$\left(\frac{\partial h}{\partial x}\right)_j^n = \left[\frac{h_{j+1}^n - h_{j-1}^n}{2\Delta X}\right] \qquad \text{(centered spatial difference using values at n)}$$

It is also possible to formulate the spatial derivatives in terms of values of h at the new time n+1.

$$\left(\frac{\partial h}{\partial x}\right)_j^n = \left[\frac{h_{j+1}^{n+1} - h_j^{n+1}}{\Delta X}\right]$$ (forward spatial difference using values at n+1)

$$\left(\frac{\partial h}{\partial x}\right)_j^n = \left[\frac{h_j^{n+1} - h_{j-1}^{n+1}}{\Delta X}\right]$$ (backward spatial difference using values at n+1)

$$\left(\frac{\partial h}{\partial x}\right)_j^n = \left[\frac{h_{j+1}^{n+1} - h_{j-1}^{n+1}}{2\Delta X}\right]$$ (centered spatial difference using values at n+1)

This listing of derivatives is not complete but is intended only to represent some simple methods of formulation. Observe that one of the major distinctions between the various derivatives is whether h^n or h^{n+1} is used in the spatial derivatives. The choice of whether to use h^n or h^{n+1} in the spatial derivative is not obvious since the derivative is to be applied over a time interval from n to n+1. Actually an average spatial derivative for this time range might appear to be most appropriate; i.e., for the forward difference

$$\left(\frac{\partial h}{\partial x}\right)_j^n = \frac{1}{2}\left[\frac{h_{J+1}^{n} - h_j^{n}}{\Delta X}\right] + \frac{1}{2}\left[\frac{h_{J+1}^{n+1} - h_j^{n+1}}{\Delta X}\right]$$

Indeed this type of information is often used.

Consider the forward time, backward difference formulation for the spatial derivative and using the values at time level n in the spatial derivatives. This formulation for the differential equation would be:

$$\left[\frac{h_j^{n+1} - h_j^n}{\Delta t}\right] + C\left[\frac{h_j^n - h_{j-1}^n}{\Delta X}\right] = 0 \qquad (16)$$

Schematically, this operation is shown in Figure 12. Using known initial data at some starting time level, n and the boundary data for all future times, the scheme uses information from one time level to compute values of the dependent variable at the next time level. To get started values of h must be defined for all x at t=0 (i.e., h(x,0) = (h(x)) and also boundary values (conditions) of h for all t at x=0(i.e., h(o,t) = h(t)). Rearranging and putting all values at the lower time level, n on the right-hand-side (RHS) of (16) gives

$$h_j^{n+1} = h_j^n - \frac{C\Delta t}{\Delta X} h_j^n + C \frac{\Delta t}{\Delta X} h_{J-1}^n \qquad (17)$$

or

$$h_j^{n+1} = (1-C_r)\, h_j^n + C_r\, h_{j-1}^n \qquad (18)$$

where

$$C_r = C \frac{\Delta t}{\Delta x} = \text{the Courant number}$$

The Courant number is the ratio of the actual physical celerity to the celerity ($\Delta x/\Delta t$) at which the numerical model propogates a disturbence.

The approximate equality (18) is an example of an explicit finite-difference scheme since any value h_j^{n+1} can be calculated directly (explicitly) from information at each preceding time level. Note the use of the boundary data at the left boundary (j-1) to keep the calculations moving ahead in time (Figure 12). This is called a "marching-type" (boundary-value) problem since we need to step-along computing all intermediate values for all grid points at each time level in order to arrive at the solution for a given future time.

Consider a different representation of the linearized wave equation using values of the velocity at the new time n+1 in the spatial derivatives. The differential equation can also be represented by:

$$\frac{h_j^{n+1} - h_j^n}{\Delta t} + C \left[\frac{h_j^{n+1} - h_{j-1}^{n+1}}{\Delta X}\right] = 0$$

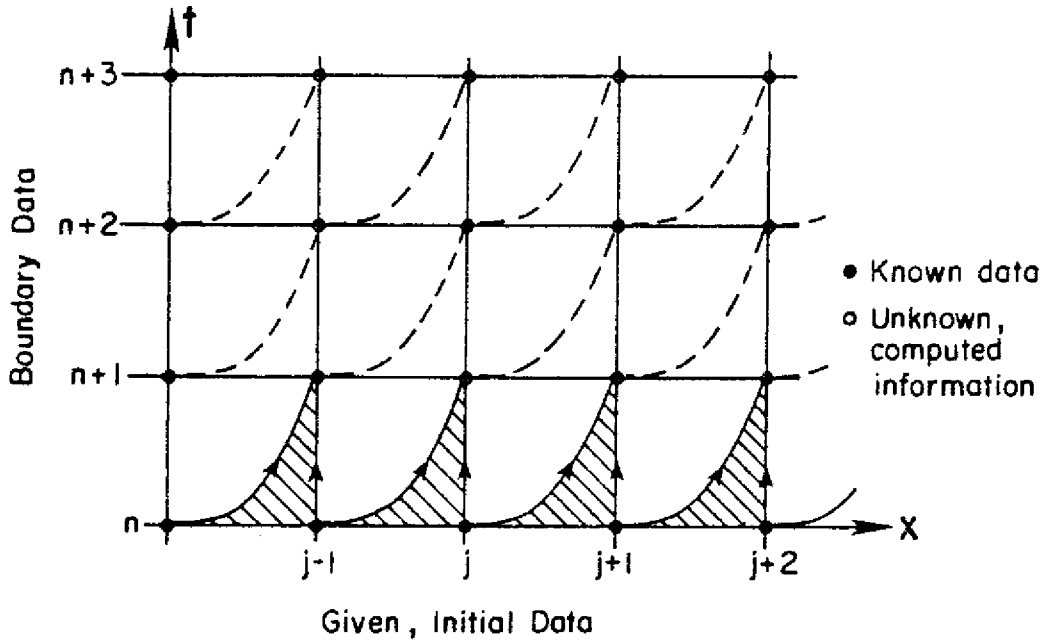

Figure 12. Schematic of F-D Scheme and Operation

What is the major difference in this formulation and the previous formulation? The inability to solve for h_j at the new time immediately in terms of known quantities. The simplified equation contains more than one unknown:

$$(1 + C\frac{\Delta t}{\Delta x})h_j^{n+1} - (C\frac{\Delta t}{\Delta x})h_{j-1}^{n+1} = h_j^n$$

This equation is of the general form:

$$C_1 h_j^{n+1} + C_2 h_{j-1}^{n+1} = h_j^n \qquad (19)$$

where C_1 and C_2 are constants.

An equation of this same general form is obtained for each cell of the system. How does one solve for the new values of h at the time level n+1? This is an example of <u>implicit formulation</u> of the problem.

A system of equations is obtained which must be solved simultaneously. Obviously the solution technique will be more involved in this case. Implicit formulations, however, have some desirable properties which may compensate for the more involved formulation and solution technique required. Numerical models formulated in this manner are called implicit models.

A combination of the explicit and implicit formulations is sometimes used in a numerical model. In this case certain variables are formulated and solved

explicitly and other variables are formulated and solved implicitly. Numerical models formulated in this way are referred to as explicit-implicit or implicit-explicit models.

These two formulations would both require retaining values of h for all cells at time n and n+1 as the calculations proceed through time. If instead of the previous formulations a centered time derivative were used, there would be 3 different times involved in the formulation n-1, n and n+1. In this case, values of h for all cells at 3 time levels would have to be retained in the computational process. The 3 time-level computational schemes obviously require more computer storage than the 2 time-level schemes; however, they have several attractive features primarily associated with being able to express time derivatives using a central difference formulation. As a result the 3 time-level finite difference computational schemes are becoming increasingly important now that larger memory computer systems are becoming more readily available.

Stability and Accuracy of Finite Difference Solutions

It is important to note that using the numerical algorithm gives a solution to the finite-difference equation and not generally to the partial differential equation from which it is modeled. Therefore,

Difference Equations ⟶ Approximate Solutions

Differential Equations ⟶ True Solutions

and how close these solutions are to one another is called numerical accuracy.

There are several ways to formulate most differential equations in terms of finite difference algorithms. Unfortunately many of the formulations will not yield satisfactory results. The choosing of the most appropriate formulations technique is one of the major problems facing an individual developing a new numerical model. As Patrick Roache indicates in his book on Computational Fluid Mechanics: "The newcomer to computational fluid dynamics is forewarned: In this field, there is as much artistry as science. -------Seemingly minor modifications of finite-difference forms, iterative schemes or boundary conditions can result in large improvements. --------One of the fascinating aspects of computational fluid dynamics is the large number of plausible schemes which do not work". These solutions schemes can generally be found in either of three categories:

(i) Inaccurate Solutions;

(ii) Accurate, (close to) True Solutions; and

(iii) Oscillating, Highly Inaccurate (unstable) Solutions.

To illustrate these three categories of solutions, again consider the linearized wave equation. The explicit forward time, backward space formulation of the equation will be considered, Equation (18).

As initial conditions for the example problem, consider the initial (t=0, i.e., n=0) flood-wave profile as having an idealized triangular shape

along the x-axis (j=1 to jj=11) and centered at grid point j=6 with scaled height, h=1.0. (See Figure 13). It is also instructive to employ periodic boundary conditions so that as the wave moves out the right-side boundary it reappears at the left-side boundary. The calculations are run for a sufficient number of time steps to cause the wave to return to its precise starting position. Since there are no friction or dispersive terms in (12), the true solution is a triangular-shaped wave which propagates from left-to-right unchanged in shape and returns to the starting position exactly as initially given. Any deviation from this result must be due to the numerical scheme and parameters employed. Taking C=1 and $\Delta x=1$,

$$C_r = C\,\frac{\Delta t}{\Delta x} \quad \text{or} \qquad \Delta t = C_r\,(\frac{\Delta x}{C}) = C_r.$$

To travel the 10 Δx distance will then require

$$nn(\Delta t) = nn(C_r) = 10 \quad (1)$$

where nn is the number of time steps. Thus for C_r = 0.5, 1.0 and 2.0, the respective values for Δt and nn are (0.5 and 20), (1.0 and 10) and (2.0 and 5).

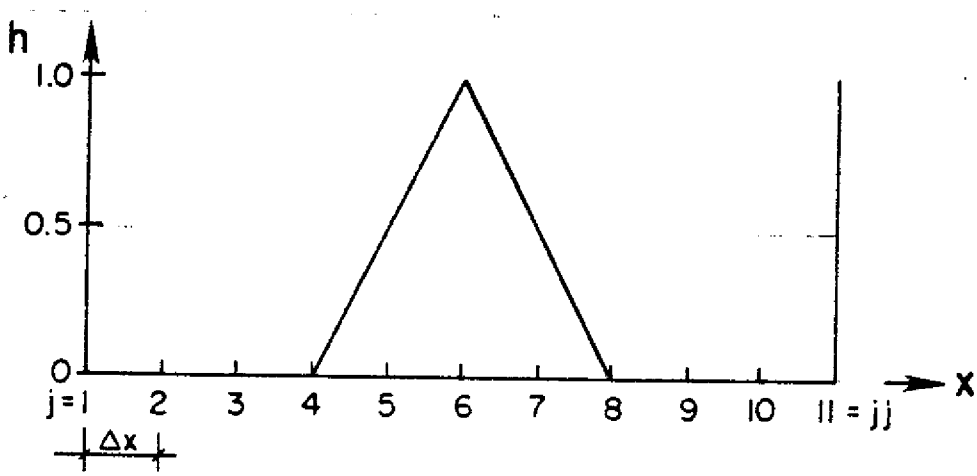

Figure 13. Initial Conditions, Triangular Flood-Wave Profile

Case 1 $C_r = 0.5$

From (18):

$$h_j^{n+1} = 0.5\,h_j^n + 0.5\,h_{j-1}^n$$

or

$$h_j^{n+1} = \left[\frac{h_j^n + h_{j-1}^n}{2}\right] \qquad (20)$$

and a few representative values can be easily calculated. The complete results are given in Table I(a) and reveal that the approximate, numerical solution is diffused in that the peak amplitude is lowered and the wave is spread out (dispersed). The wave peak remains in its proper position in time so that the phase of the wave appears okay. This is an example of numerical amplitude dispersion and the solution must be regarded as poor and inaccurate.

Case 2 $C_r = 1.0$

Equation (18) now gives $h_j^{n+1} = h_{j-1}^n$ and Table I(b) shows the initial wave shape propagating and undisturbed as the solution surface and returning exactly as it began to the starting position. This is identical to the exact solution so that our approximation is the best possible in this case.

Case 3 $C_r = 2.0$

Putting $C_r = 2.0$ in (18) gives

$$h_j^{n+1} = -h_j^n + 2h_{j-1}^n \tag{21}$$

and all computed results are shown in part (c), Table I. Oscillations set-in and the result at T=10 bears no resemblance to the true solution. Such a computation is completely useless for practical purposes. This oscillating "solution" will continue to get worse as time increases and the difference scheme with C_r (i.e., $\Delta t/\Delta x$) so chosen is unstable.

All results at T=10 from Table I have been plotted in Figure 14 to demonstrate the basic solution categories described above, i.e.,

(i) Inaccurate, Case 1,

(ii) Accurate, True Solutions, Case 2, and

(iii) Oscillating, Unstable Solutions, Case 3.

Hence, accuracy is closely related to stability, Case 1 was stable, yet very inaccurate. In summary, to have the "best" approximation one must:

1. use the "best finite-difference scheme";

2. use an optimal $C_r = C\Delta t/\Delta x$ to give optimal, yet stable conditions;

3. use "efficient" algorithms with regards to programming ease, calculation time (CPU, times) and storage space on the computer.

Taking the true celerity, C equal to 1.0 in the above examples, resulted in $C_r = \Delta t/\Delta x = 0.5$, 1.0, and 2.0. This parameter is seen to play an important role in the basic solution category for the finite difference equation.

TABLE I. Results of Example Calculations

(a) Case 1 $C_r = 0.5$ ($\Delta t = 0.5$, nn = 20, $T = (nn)(\Delta t) = 10$)

$$h_j^{n+1} = \left[\frac{h_j^n + h_{j-1}^n}{2}\right]$$

TIME STEPS											
NN=20	.070	.091	.155	.237	.308	.336	.308	.237	.115	.091	.070
19	.070	.113	.194	.280	.336	.336	.280	.194	.113	.070	.070
18	.082	.149	.240	.320	.352	.320	.240	.149	.082	.059	.082
17	.106	.192	.288	.352	.352	.288	.192	.106	.059	.059	.106
16	.142	.242	.334	.371	.334	.242	.142	.011	.046	.071	.142
15	.188	.297	.371	.371	.297	.188	.096	.046	.046	.096	.188
14	.244	.349	.393	.349	.242	.134	.059	.033	.058	.133	.244
13	.305	.393	.393	.305	.183	.084	.033	.033	.084	.183	.305
12	.366	.419	.366	.244	.122	.045	.021	.045	.122	.244	.366
11	.419	.419	.314	.174	.070	.021	.021	.070	.175	.314	.419
10	.451	.387	.242	.107	.032	.011	.032	.107	.242	.387	.451
9	.451	.322	.161	.054	.011	.011	.054	.161	.322	.451	.451
8	.410	.234	.088	.019	.004	.019	.088	.234	.410	.492	.410
7	.328	.141	.035	.004	.004	.035	.141	.328	.492	.492	.328
6	.219	.062	.008	.000	.008	.062	.219	.437	.547	.437	.219
5	.109	.015	.000	.000	.015	.109	.328	.547	.547	.328	.109
4	.031	.000	.000	.000	.031	.187	.468	.625	.468	.187	.031
3	.000	.000	.000	.000	.062	.312	.625	.625	.312	.062	.000
2	.000	.000	.000	.000	.125	.000	.750	.500	.125	.000	.000
1	.000	.000	.000	.000	.250	.750	.750	.250	.000	.000	.000
0	.000	.000	.000	.000	.500	1.000	.500	.000	.000	.000	.000
	J=1	2	3	4	5	6	7	8	9	10	11=JJ

TABLE I. (continued)

(b) Case 2 C_r = 1.0 (Δt = 1.0, nn = 10, T = (nn)(Δt) = 10)

$$h_j^{n+1} = h_{j-1}^n$$

NN=												
TIME STEPS	10	.000	.000	.000	.000	.500	1.000	.500	.000	.000	.000	.000
	9	.000	.000	.000	.500	1.000	.500	.000	.000	.000	.000	.000
	8	.000	.000	.500	1.000	.500	.000	.000	.000	.000	.000	.000
	7	.000	.000	1.000	.500	.000	.000	.000	.000	.000	.000	.000
	6	.500	1.000	.500	.000	.000	.000	.000	.000	.000	.000	.500
	5	1.000	.500	.000	.000	.000	.000	.000	.000	.000	.500	1.000
	4	.500	.000	.000	.000	.000	.000	.000	.000	.500	1.000	.500
	3	.000	.000	.000	.000	.000	.000	.000	.500	1.000	.500	.000
	2	.000	.000	.000	.000	.000	.000	.000	1.000	.500	.000	.000
	1	.000	.000	.000	.000	.000	.500	1.000	.500	.000	.000	.000
	0	.000	.000	.000	.000	.500	1.000	.500	.000	.000	.000	.000
		J=1	2	3	4	5	6	7	8	9	10	11=JJ

(c) Case 3 C_r = 2.0 (Δt = 2.0, nn = 5, T = (nn) (Δt) = 10)

$$h_j^{n+1} = -h_j^n + 2h_{j-1}^n$$

NN=												
TIME STEPS	5	-8.000	16.000	.000	.000	-.500	4.000	-10.500	5.000	20.000	-24.000	-8.000
	4	8.000	.000	.000	.000	.500	-3.000	4.500	4.000	-12.000	.000	8.000
	3	.000	.000	.000	.000	-.500	2.000	-.500	-5.000	7.000	4.000	.000
	2	.000	.000	.000	.000	.500	-1.000	-1.500	2.000	2.000	.000	.000
	1	.000	.000	.000	.000	-.500	.000	1.500	1.000	.000	.000	.000
	0	.000	.000	.000	.000	.500	1.000	.500	.000	.000	.000	.000
		J=1	2	3	4	5	6	7	8	9	10	11=JJ

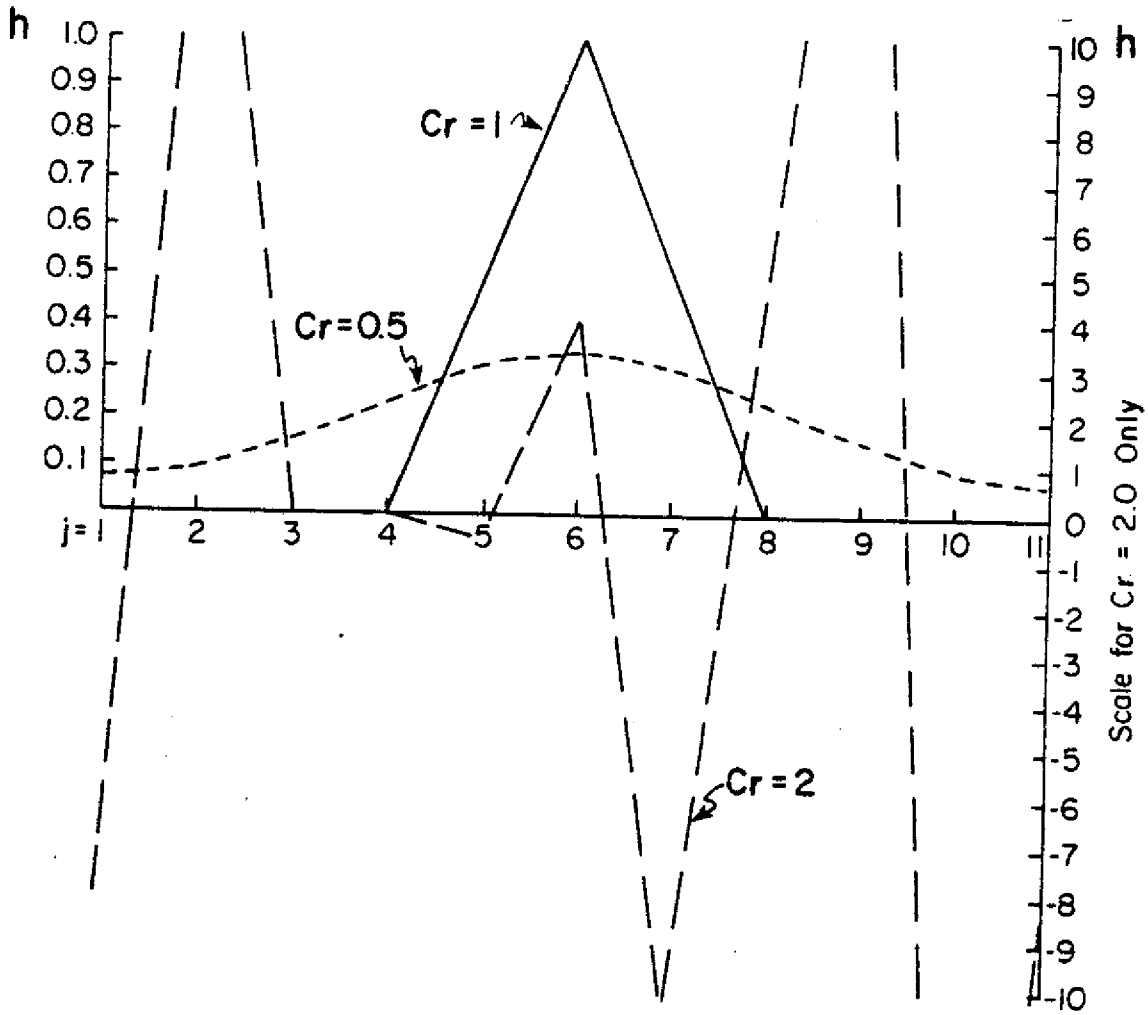

Figure 14. Comparison of Cases After Wave Return to Initial Position

Consistency and Convergence of Finite Difference Equations

The Taylor series is a fundamental tool of numerical methods. With it the truncation errors of any discrete, finite-difference analog of the continuum partial differential equations can be determined. How these analog equations tend to zero as the grid cells are reduced in size indicates the consistency of the scheme. Consider the finite difference representation of the linearized wave equation given by Equation (16).

$$\left[\frac{h_j^{n+1} - h_j^n}{\Delta t}\right] + C\left[\frac{h_j^n - h_{j-1}^n}{\Delta x}\right] = 0 \qquad (16)$$

Expand the values of h at time level n+1 and spatial location j-1 using a Taylor series to obtain:

$$h_{j-1}^{n} = h_j^n + \left(\frac{\partial h}{\partial X}\right)_j^n (-\Delta X) + \left(\frac{\partial^2 h}{\partial X^2}\right)_j^n \frac{(-\Delta X)^2}{2!} + \left(\frac{\partial^3 h}{\partial X^3}\right)_j^n \frac{(-\Delta X)^3}{3!} + \text{H.O.T.} \qquad (22)$$

and

$$h_j^{n+1} = h_j^n + \left(\frac{\partial h}{\partial t}\right)_i^n \Delta t + \left(\frac{\partial^2 h}{\partial t^2}\right)_i^n \frac{\Delta t^2}{2!} + \left(\frac{\partial^3 h}{\partial t^3}\right)_i^n \frac{\Delta t^3}{3!} + \text{H.O.T.} \qquad (23)$$

Putting (22) and (23) into (16) gives

$$h_j^n + \left(\frac{\partial h}{\partial t}\right)_j^n \Delta t + \left(\frac{\partial^2 h}{\partial t^2}\right)_j^n \frac{\Delta t^2}{2!} + \left(\frac{\partial^3 h}{\partial t^3}\right)_j^n \frac{\Delta t}{3!} + \text{H.O.T.}$$

$$= h_j^n - \frac{C\Delta t}{\Delta X} h_j^n + C\frac{\Delta t}{\Delta X}\left[h_j^n - \left(\frac{\partial h}{\partial X}\right)_j^n \Delta X + \left(\frac{\partial^2 h}{\partial X^2}\right)_j^n \frac{\Delta X}{2!} - \left(\frac{\partial^3 h}{\partial X^3}\right)_j^n \frac{\Delta X^3}{3!} + \text{H.O.T.}\right.$$

Cancelling similar terms and dividing thru by Δt gives

$$\left(\frac{\partial h}{\partial t}\right)_j^n + \left(\frac{\partial^2 h}{\partial t^2}\right)_j^n \frac{\Delta t}{2!} + \left(\frac{\partial^3 h}{\partial t^3}\right)_j^n \frac{\Delta t^2}{3!} + \text{H.O.T.}$$

$$= -C\left(\frac{\partial h}{\partial X}\right)_j^n + C\left(\frac{\partial^2 h}{\partial X^2}\right)_j^n \frac{\Delta X}{2!} - C\left(\frac{\partial^3 h}{\partial X^3}\right)_j^n \frac{\Delta X^2}{3!} + \text{H.O.T.}$$

All terms are for any arbitrary point (j,n) so the subscript and superscript notation can now be dropped. Rearranging terms yields:

$$\frac{\partial h}{\partial t} + C\frac{\partial h}{\partial X} + \overbrace{\left[\frac{\partial^2 h}{\partial t^2}\frac{\Delta t}{2!} - C\frac{\partial^2 h}{\partial X^2}\frac{\Delta X}{2} + \frac{\partial^3 h}{\partial t^3}\frac{\Delta t^2}{3!} + C\frac{\partial^3 h}{\partial X^3}\frac{\Delta X^2}{3!} + \text{H.O.T.}\right]}^{\text{-TRUNCATION ERROR-}} = 0 \qquad (24)$$

Thus by using the Taylor series in the finite difference scheme the original partial differential equation is recovered plus additional terms which are the truncation errors for the scheme given by Equation (16). Observe that as the grid is shrunk and Δt, $\Delta x \to 0$, then the finite difference scheme reduces to the partial differential equation. Also, there are no constraints or conditions required on how the grid is shrunk so that the finite difference equation is unconditionally consistent with the partial differential equation. The truncation errors are of order $O(\Delta t, \Delta x)$ since these are the lowest order terms occurring. If only terms of $O(\Delta t^2, \Delta x^2)$ appeared then the truncation errors would disappear faster as Δt, $\Delta x \to 0$. This would be a higher order scheme. Truncation errors are ultimately responsible for differences between numerical and continuum solutions and should not be confused with machine round-off errors. The term consistency deals with relations between equations in their continuum versus discrete forms.

Convergence is a familiar mathematical expression related to whether (or how) solutions of discrete, finite-difference analogs approach the true solution of the continuum, differential equation. Thus convergence deals with relations between solutions as Δt, $\Delta x \to 0$. If the sequence of solutions tends to the true solution as Δt, $\Delta x \to 0$, then the solution of the difference scheme is convergent. Using the triangle-wave example and the now familiar finite difference scheme given by Equation (16), some approximate solutions are computed for shrinking Δt and Δx to study the convergence concept. The ratio $C\Delta t/\Delta x$, i.e., the Courant number is kept constant during the grid shrinking process for convenience in comparing these results with those previously shown.

Case 1 $C_r = 0.5$

Initially consideration was given to $\Delta t = \frac{1}{2}$, $\Delta x = 1$. Now consider $\Delta t = \frac{1}{4}$, $\Delta x = \frac{1}{2}$; then $\Delta t = 1/8$, $\Delta x = \frac{1}{4}$, etc. The results plotted in Figure 15 clearly reveal how solutions are converging toward the true solution as Δt, $\Delta x \to 0$. In this case the accuracy improves as the grid is shrunk.

Case 2 $C_r = 1.0$

This solution was exact and involved no truncation errors.

Case 3 $C_r = 2.0$

Before,consideration was for $\Delta t = 2$, $\Delta x = 1$. Now consider $\Delta t = 1$, $\Delta x = \frac{1}{2}$, etc., gradually shrinking both Δt and Δx proportionately. The approximation becomes progressively worse (Figure 16) since stronger oscillations appear as Δt, $\Delta x \to 0$. The solution becomes more unstable and accuracy rapidly deteriorates as the grid is shrunk. Convergence, stability and accuracy are closely linked. Observe that for a stable solution the accuracy is increased by reducing Δt and Δx. It is incorrect, however, to believe that numerical instability problems can be removed or accuracy increased simply by using a finer mesh. As demonstrated by the example, the relation between flow parameters and grid scales Δt, Δx is important for stability and accuracy. In our case the Courant number is the important parameter. Other equations will have similar parameters.

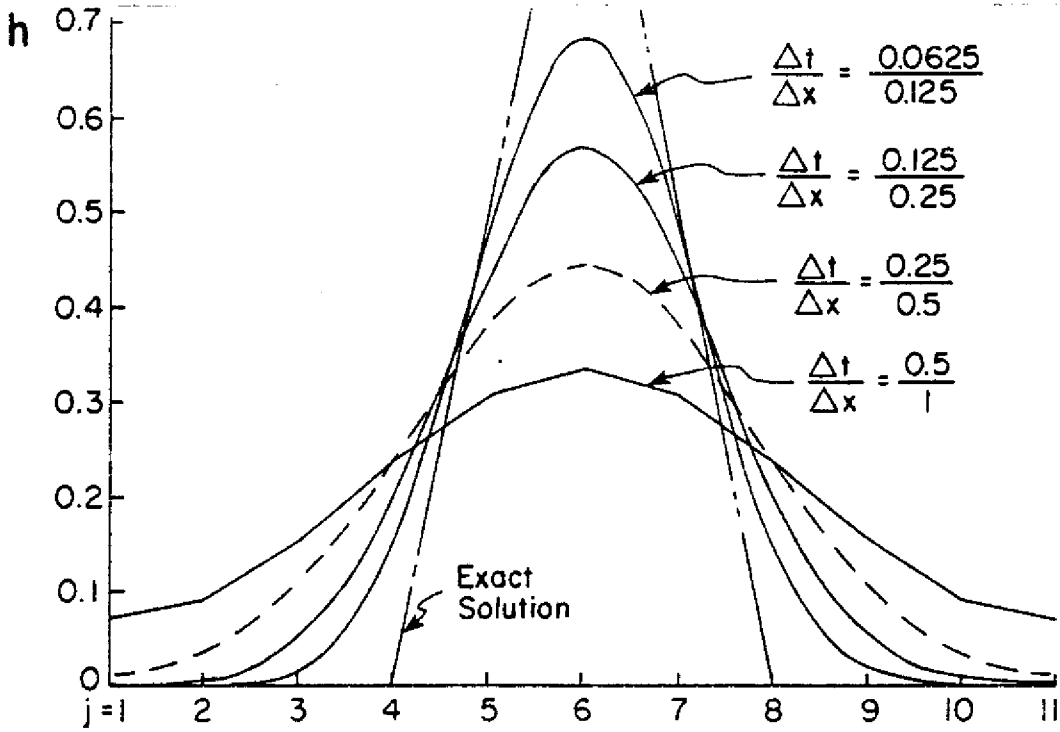

Figure 15. Effects of Grid Shrinking, $C_r = 0.5$

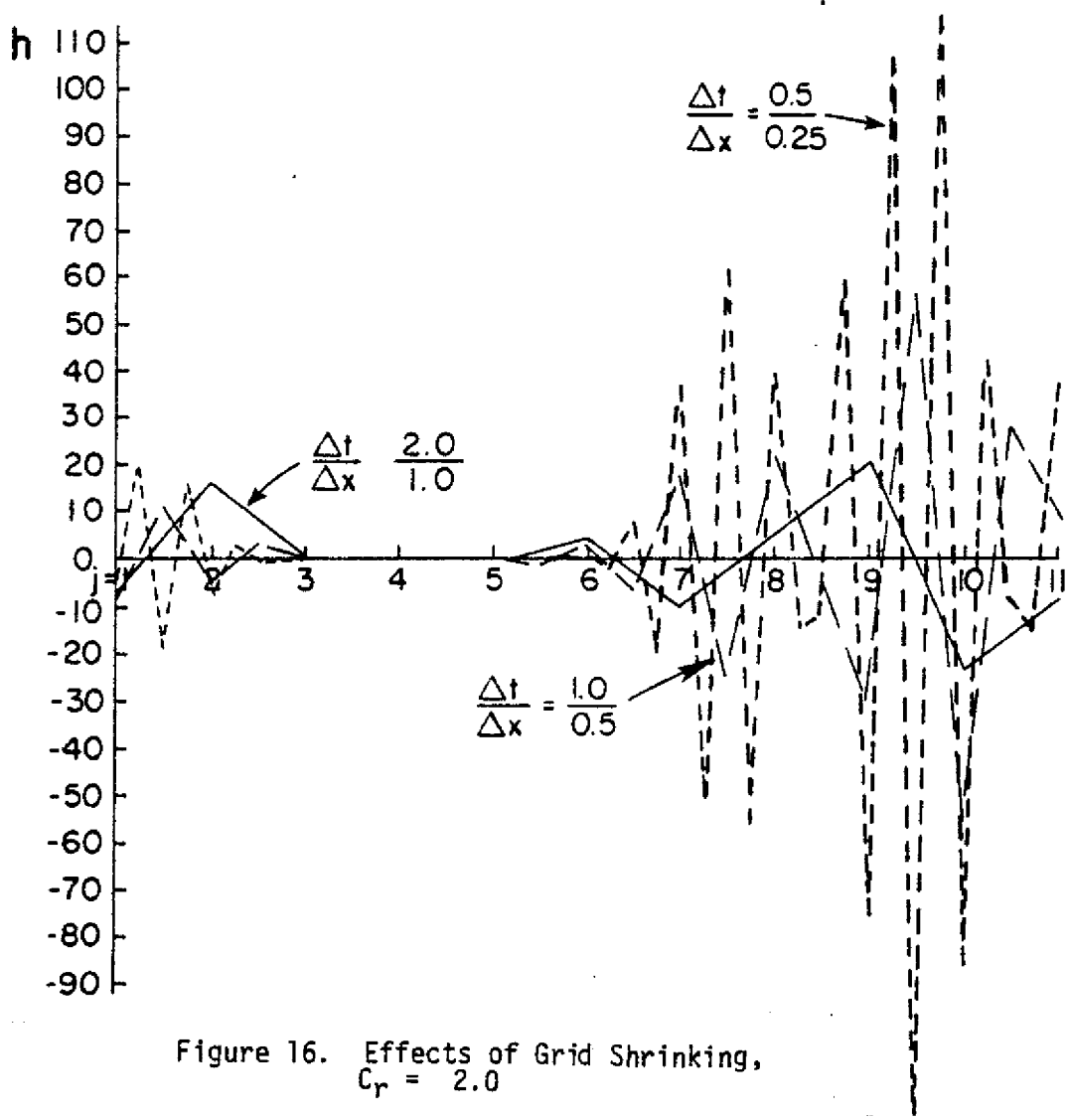

Figure 16. Effects of Grid Shrinking, $C_r = 2.0$

Basic Model Types

The governing equations for the generalized three-dimensional flow of a fluid represent a complex system of non-linear partial differential equations. A typical set of equations might be represented by:

CONTINUITY EQUATION

$$\frac{\partial \rho}{\partial t} + \frac{\partial}{\partial x}(\rho u) + \frac{\partial}{\partial y}(\rho v) + \frac{\partial}{\partial z}(\rho w) = 0$$

MOMENTUM EQUATIONS

$$\frac{\partial u}{\partial t} + u\frac{\partial u}{\partial x} + v\frac{\partial u}{\partial y} + w\frac{\partial u}{\partial z} - fv = -\frac{1}{\rho}\frac{\partial p}{\partial x} + \frac{k}{\rho}\left(\frac{\partial^2 u}{\partial x^2} + \frac{\partial^2 u}{\partial y^2} + \frac{\partial^2 u}{\partial z^2}\right)$$

$$\frac{\partial u}{\partial t} + u\frac{\partial v}{\partial x} + v\frac{\partial v}{\partial y} + w\frac{\partial v}{\partial z} + fu = -\frac{1}{\rho}\frac{\partial p}{\partial y} + \frac{k}{\rho}\left(\frac{\partial^2 v}{\partial x^2} + \frac{\partial^2 v}{\partial y^2} + \frac{\partial^2 v}{\partial z^2}\right) \qquad (25)$$

$$\frac{\partial w}{\partial t} + u\frac{\partial w}{\partial x} + v\frac{\partial w}{\partial y} + w\frac{\partial w}{\partial z} = -\frac{1}{\rho}\frac{\partial p}{\partial z} + \frac{k}{\rho}\left(\frac{\partial^2 w}{\partial x^2} + \frac{\partial^2 w}{\partial y^2} + \frac{\partial^2 w}{\partial z^2}\right)$$

The formulation and calculation process for a three-dimensional numerical model is involved. In addition, three-dimensional models require a large quantity of prototype data for the verification and calibration process.

Fortunately many hydrodynamic events can be satisfactorily represented by a simplified system of governing equations, rather than the generalized three-dimensional equations. For example, for flow in a river, only the river elevation and the volumetric flow rate passing a point at any time may be of interest. Thus, only one spatial dimension is involved. This type problem is illustrated in Figure 17. This problem can be formulated so that only the variables Q (flow rate) and h (surface elevation) are dependent variables in the problem. A system of two equations, one momentum equation and the continuity equation, are required to be solved to obtain a solution of Q and h. This type problem would obviously have fewer finite difference cells and would be much simpler to solve than the general three-dimensional system of equations. This solution will also fail to provide any detailed variation of the velocity with depth or the velocity variation across the river. However, if only flow rate and surface elevations are of interest, then a satisfactory solution can be obtained from this model. This type model is relatively inexpensive to operate and verify.

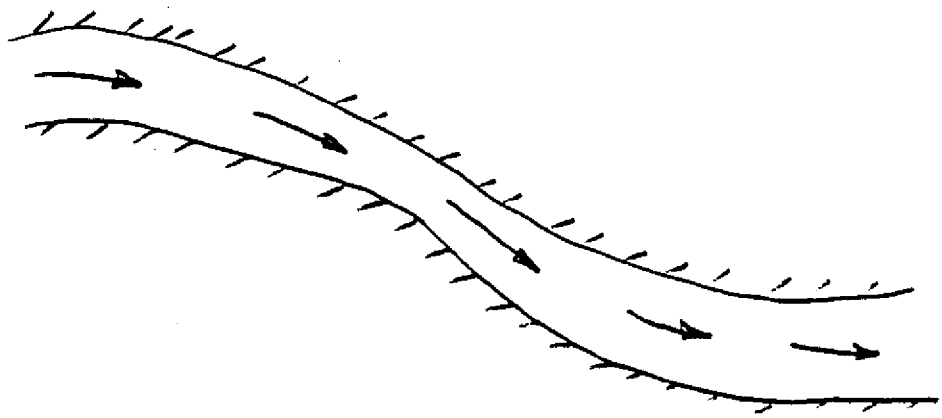

Figure 17. One-Dimensional Flow in a River

There is also a category of problems where the essential character of the flow is two-dimensional. This problem is best illustrated by the unstratified tidal circulation problem. For tidal circulation flow in an estuary or harbor, obviously the flow varies with position in the harbor. However, as illustrated in Figure 18, in many cases there is relatively little variation of flow across the depth of the water column and an average velocity over the depth has some physical significance. This problem can thus be formulated as a two-dimensional flow expressed in terms of U, V and h, where U and V are average x and y components of velocity obtained by averaging the velocity over the water depth. This problem will involve two momentum equations and the continuity equation. The problem is still much simpler to formulate, operate and verify than the general three-dimensional flow problem. At the same time, for those problems where the velocity does not vary greatly over depth very satisfactory results can be obtained.

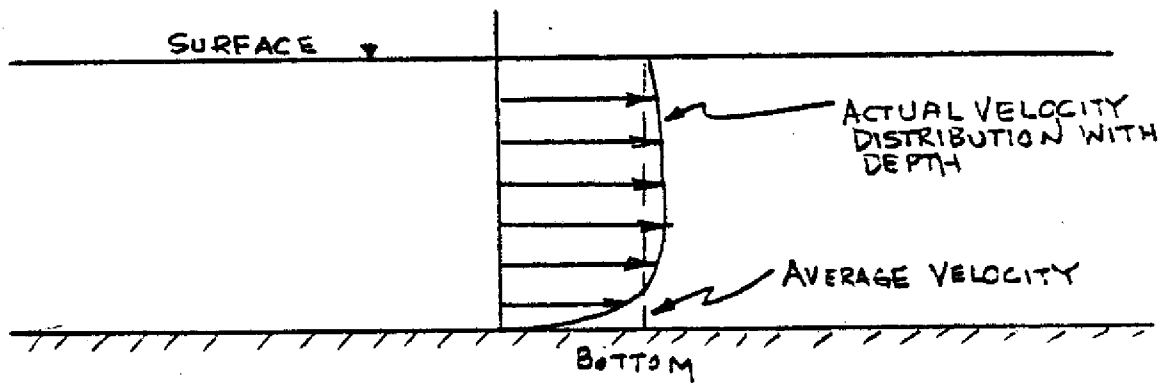

Figure 18. Typical Velocity Distribution Across the Water Depth for Unstratified Tidal Circulation

The three-dimensional model is the most involved. A three-dimensional array of cells is required. There are, however, certain problems where it is necessary to use a three-dimensional model to satisfactorily define the flow field. For example, circulation in a lake is primarily due to wind stress. The surface velocity in the lake is thus basically in the same direction as the wind. The velocity, however, varies greatly with depth and indeed the bottom velocity in the lake may be essentially opposite in direction to the wind. This is illustrated in Figure 19. Obviously an average velocity over the depth has little physical relationship to the actual velocity distribution. Three-dimensional models require large numbers of finite difference cells, the calculation procedure is involved and the model is difficult to verify.

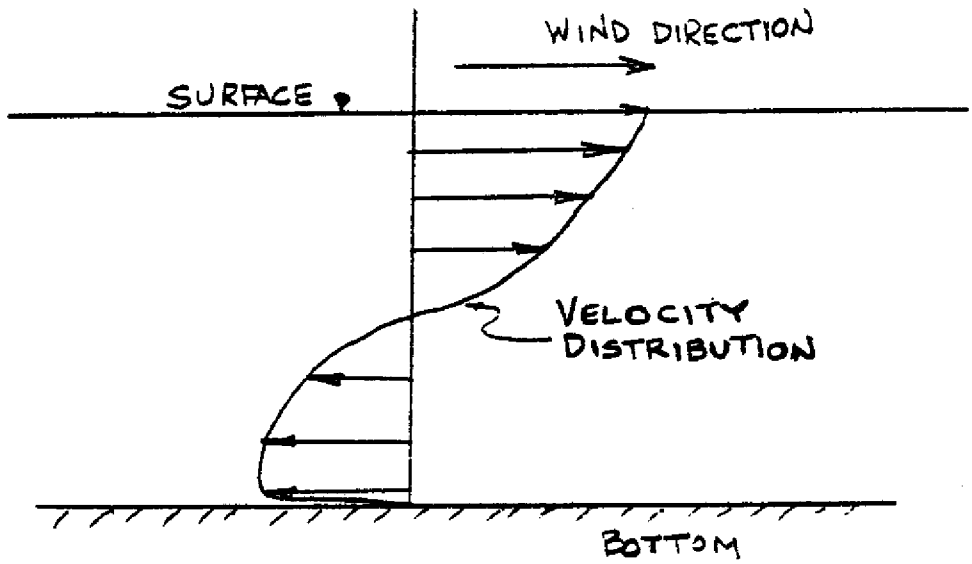

Figure 19. Typical Velocity Distribution in a Lake

The simplest model which will yield satisfactory results should be used in any modeling effort. Obviously a three-dimensional model could be applied to a problem which is basically one-dimensional. However, if Q (flow rate) and h (surface deformation) are really all that is important, use of a three-dimensional model would not be justified.

Finite Difference Grid and Boundary Conditions for Numerical Hydrodynamic Models

Consider applying a two-dimensional finite difference model to the lake as shown in Figure 20. The first consideration is to determine an appropriate finite difference grid, one which allows the satisfactory representation of important physical features of the body of fluid. This process involves subdividing the entire body of water into distinct cells as illustrated in Figure 21. The appropriate "cell" size is determined based upon a number of considerations. Among the factors to be considered are:

1. The regularity or irregularity of the shoreline.
2. The width and regularity of any channels.

3. The size and position of physical features such as weirs, breakwaters, etc., which must be simulated.
4. The desired accuracy of the model.
5. The available computer facility.
6. The available funds and time for the modeling effort.

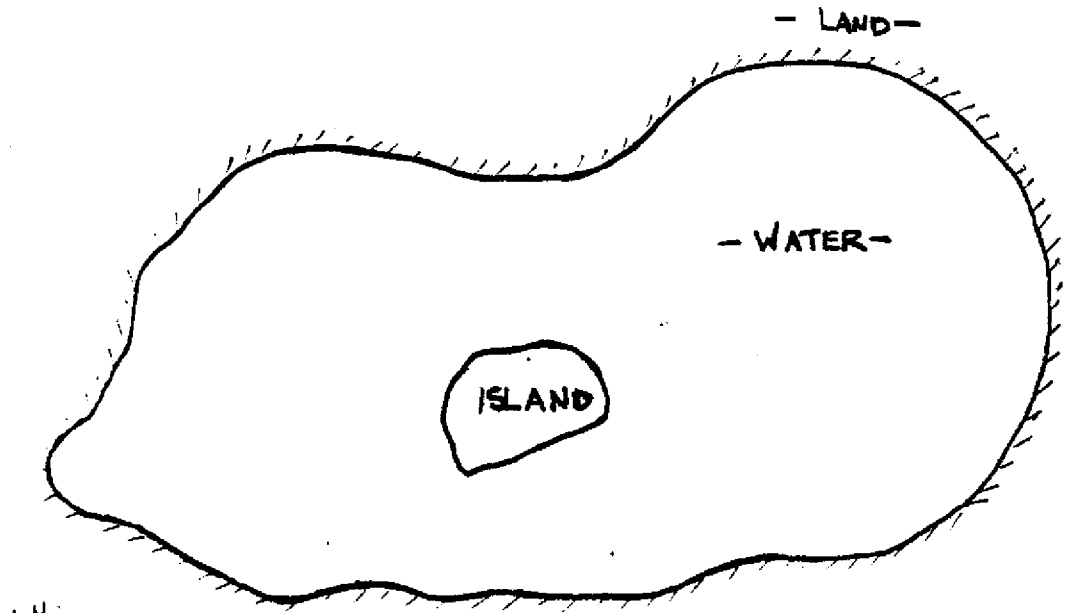

(a) Physical System

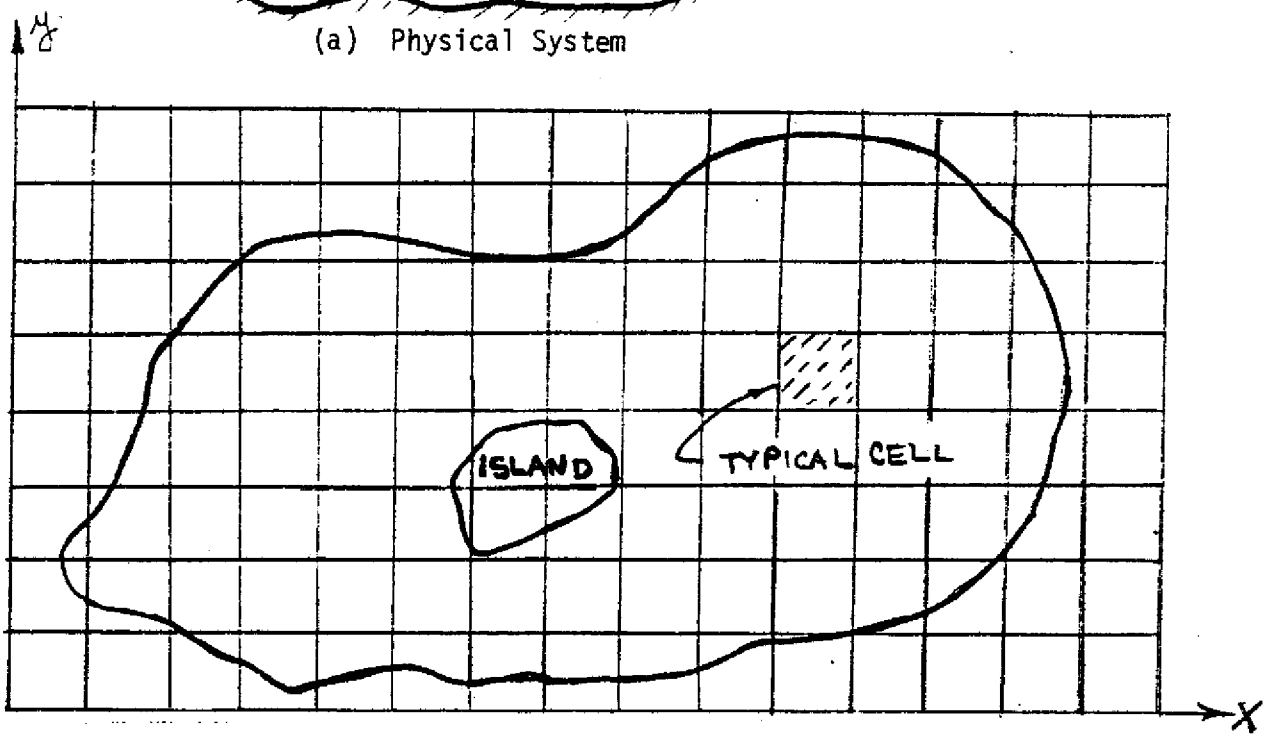

(b) Finite Difference Grid Positioned on Physical System

Figure 20. Two-Dimensional Finite Difference Grid Positioned on a Body of Fluid

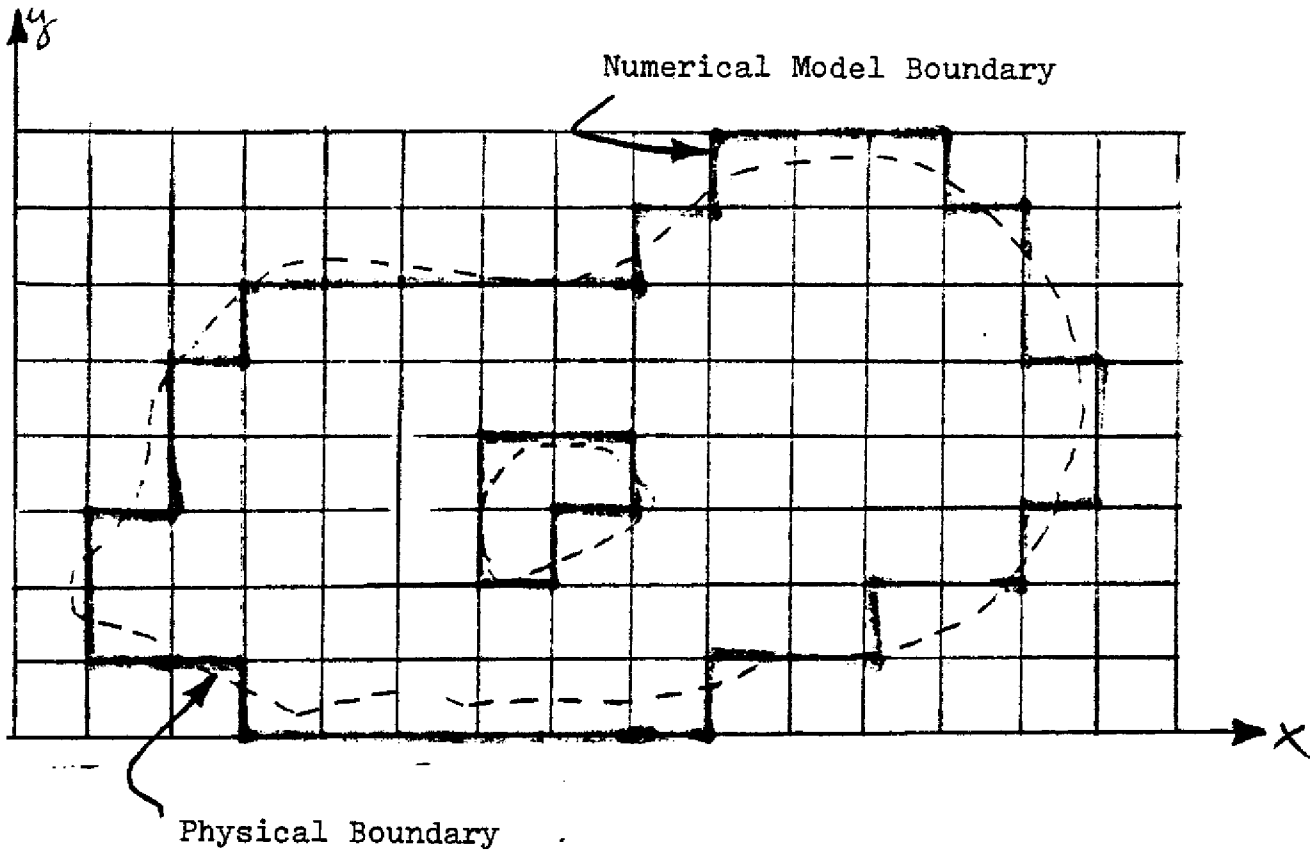

Figure 21. Two-Dimensional Finite Difference Representation of a Body of Fluid

In Figure 21 is illustrated a two-dimensional finite difference grid representation of a body of fluid. The dotted line indicates the actual boundary of the body of fluid while the heavy solid line represents the numerical representation of the body of fluid. With finite difference techniques one is normally limited to rectangular cells and the shoreline must be approximated by a sequence of straight line segments. One must keep in mind that the numerical model solves for the system bounded by the heavy solid lines not the actual physical system. The model solution can represent a solution to the actual system only to the extent that the finite difference grid approximates the actual physical system. Obviously, as illustrated in Figure 22, a smaller size finite difference cell will allow a better representation of the physical system. Of course, the same is true of an island in the body of fluid. The smaller grid and better representation is obtained, however, at the expense of having a larger number of cells with which to work. This increases the computer time required to simulate the physical phenomenon as well as greatly increasing the amount of initial input data required for the model.

Every finite difference cell in the two-dimensional finite difference grid of Figure 23 will typically require initial data giving the depth of water for the cell, the frictional characteristic of the bottom material,

whether the cell is land or water and possibly other data. As the numerical simulation proceeds, the two-dimensional velocity components u and v and surface elevation h are calculated (along with possibly other variables) for every cell at each time level at which calculations are performed.

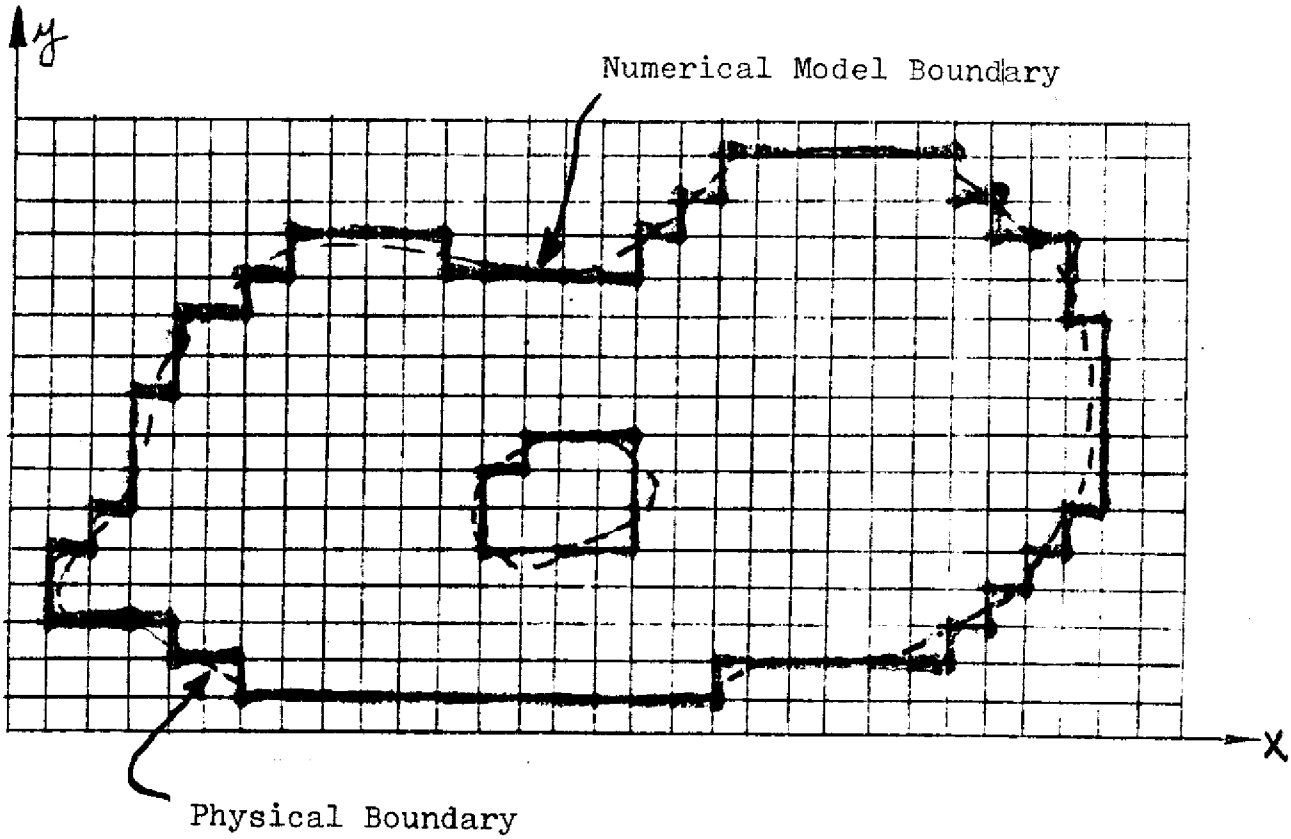

Figure 22. Finite Difference Representation of a Body of Fluid (Using a Smaller Cell Size than in Figure 21)

Regions where the depth varies significantly, such as a dredged channel, may require a small cell size to represent the channel satisfactorily. Since each cell has a depth associated with it you have a problem similar to that at the boundaries. This is illustrated in Figure 23.

Some models have the capability to vary the cell size so that a large cell size can be used whenever possible but with the capability of making the cell size small in regions where it is required for proper resolution of physical detail. This is illustrated in Figures 24 and 25.

The formulation problems for the variable cell size models are more difficult but it economizes on the amount of computer time and input data required to simulate a particular problem to a given degree of accuracy.

Of course, the maximum total number of cells which can be used in a numerical modeling effort may be limited by the size memory in the available digital computer. Each cell requires several memory locations for input data and calculated results. The speed of the computer may also impact on the

total number of cells which will be feasible for a study. Monetary and time constraints also limit the size and number of cells which can be used.

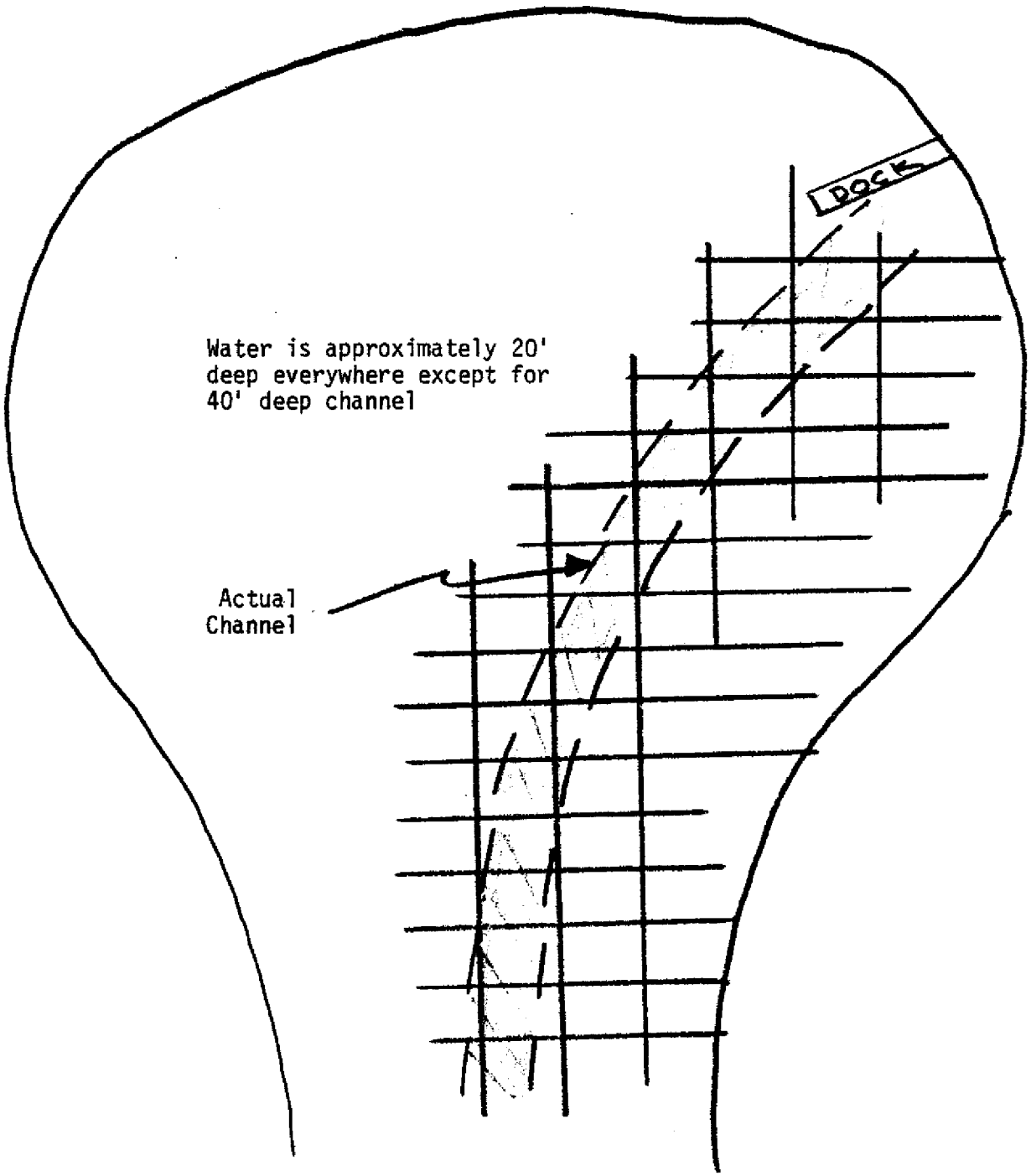

Figure 23. Representation of a Channel in a Fluid Body

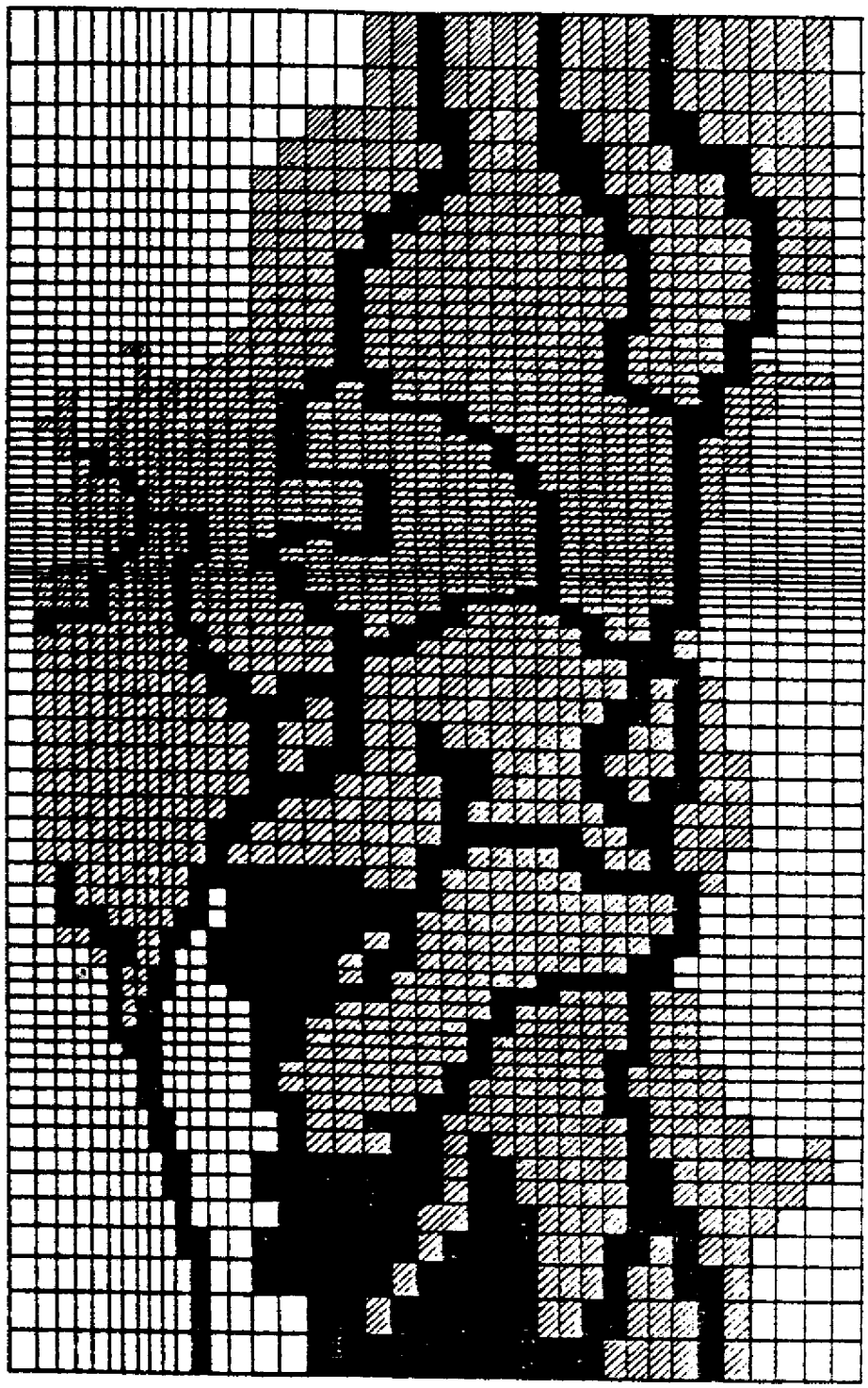

Figure 24. Illustration of a Variable Cell Size Finite Difference Grid (Mobile Bay Delta Region)

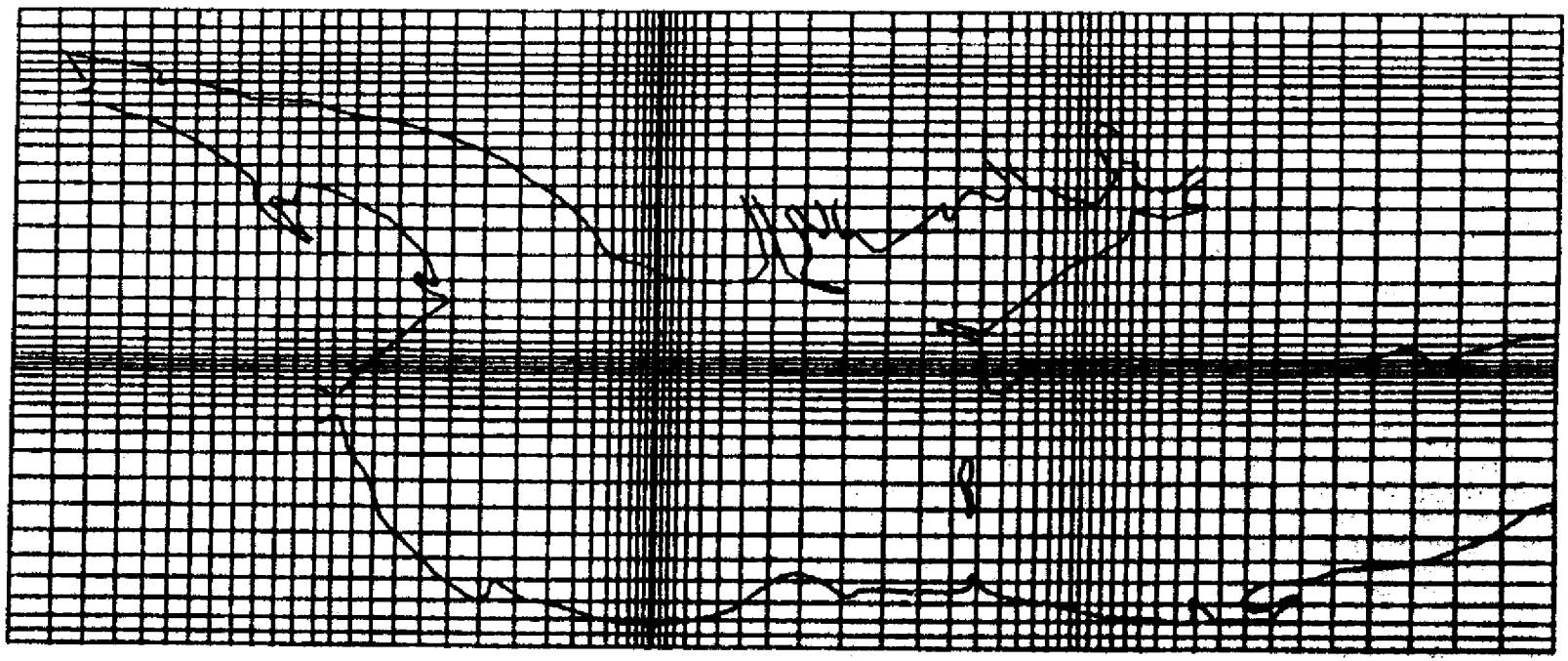

Figure 25. Illustration of a Variable Cell Size Finite Difference Grid (Apalachicola Bay).

In most numerical models the program variables are defined at staggered locations in the cells as illustrated in Figure 26 (a) rather than at a central location as shown in Figure 26 (b). Defining the variables in this manner facilitates imposing boundary conditions and formulating derivatives. For example, in Figure 27 there is illustrated a cell adjacent to a land boundary on one side. With the staggered definition of variables, the boundary condition u = 0 at the land boundary is readily apparent. Also with the velocity components as indicated in Figure 27 the derivative ∂u/∂x for the shaded cell can be readily formulated as:

$$\frac{\partial u}{\partial x} = \left[\frac{u_B - u_A}{\Delta x}\right]$$

This is illustrated in Figure 27. This derivative for the cell is much more apparent than would be the case if the velocity components were defined at the center of the cell. A similar situation exists for other terms and derivatives which occur in the governing finite difference equation.

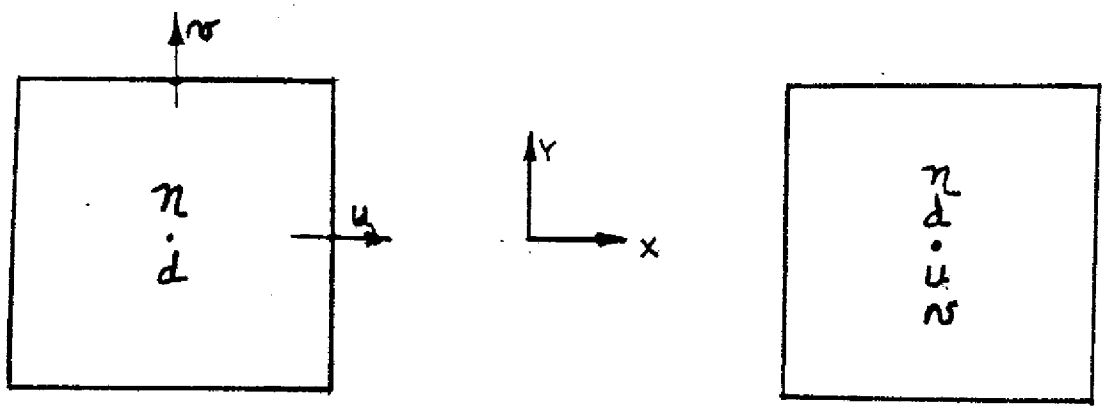

Staggered Definition of Variables

Central Definition of Variables

Figure 26. Variable Definition in Finite Difference Cells

Most of the principles discussed in the previous paragraphs for two-dimensional models also apply to one and three-dimensional models. The specific details may vary but the same general concepts are valid for all finite difference models regardless of the number of spatial dimensions involved.

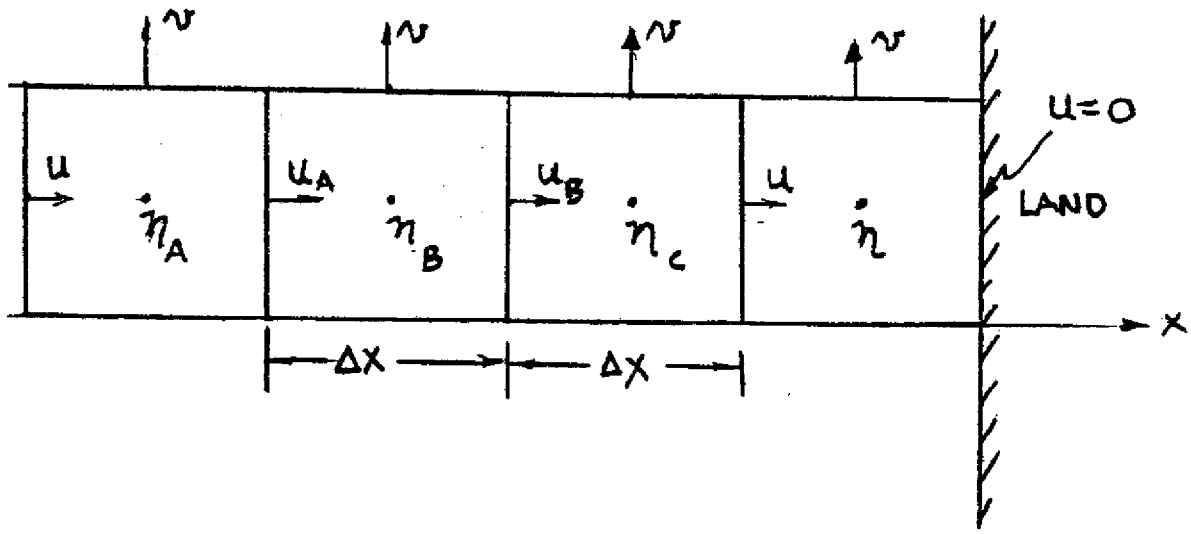

Figure 27. Cell Velocity Boundary Condition

Calibration and Verification of Finite Difference Models

Finite difference models must be calibrated and verified before they can be used with confidence as a predictive tool. The process of calibration consists of adjusting model parameters such as bottom friction, depths, etc. to bring the numerical model into agreement with prototype data. Once the model has been "tuned" or verified, these model parameters should not change significantly for similar operating conditions. Verification consists of applying the calibrated model for a second set of prototype data and demonstrating that the model correctly predicts the system behavior for this different set of boundary conditions. The model can then be used to predict potential changes associated with proposed modifications to the physical system.

Typical model calibration curves are shown in Figure 28. This type calibration would be necessary at a number of points in the system to insure that the numerical model is properly describing the system behavior.

Model Application

An application of a two dimensional depth averaged finite difference model is presented in Appendix A. This model application is an investigation of the effects on flood stage elevations produced by a railroad, built on a fill, crossing the flood plains above Mobile Bay.

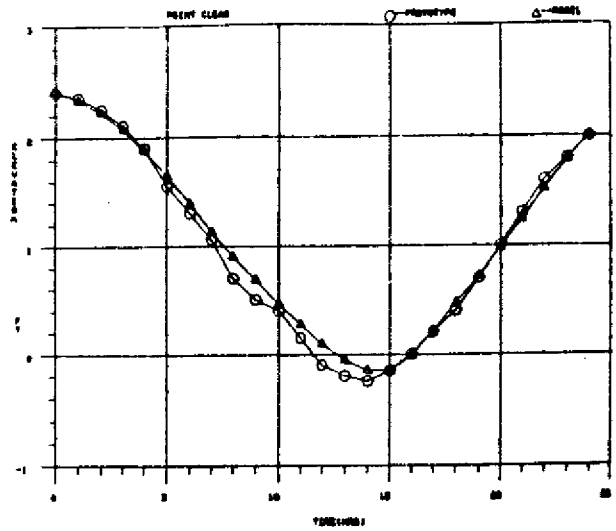

Tidal Elevation Comparison at
Point Clear

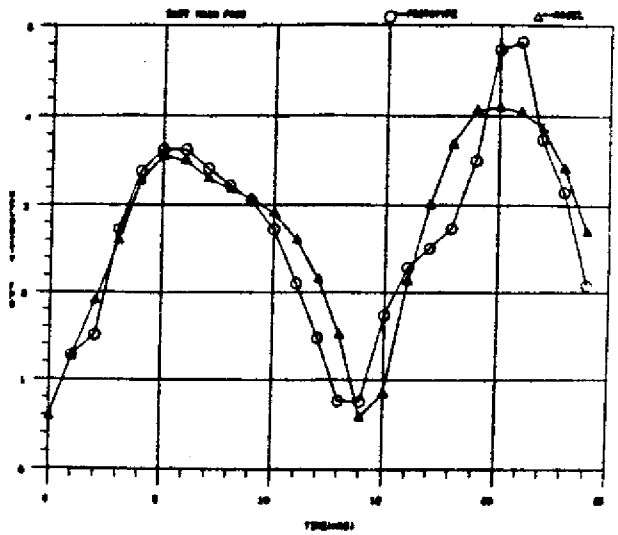

Velocity Comparison at East Pass

Figure 28. Typical Model Calibration Curves

References

Roache, Patrick J., "Computational Fluid Dynamics", Hermosa Publishing, Albuquerque, New Mexico, 1972.

Abbott, M. B., "Computational Hydraulics", Pitman Publishing Limited, London, 1979.

Basco, David R., "Notes for Short Course on Computational Hydraulics", Texas A&M University, May 26-28, 1980.

APPENDIX A

NUMERICAL COMPUTATIONS FOR ESTUARINE FLOOD PLAINS

By Donald C. Raney[1], John N. Youngblood[2] and Hasan Urgun[3]

INTRODUCTION

Freshwater inflow, an essential component of estuaries, can produce significant problems during periods of large inflow. The highly variable nature of many estuarine river systems, the geometry, topography, and bathmetry of the estuary and the interaction of local winds and astronomical tides produce a hydraulically complex environment. Man's tendency to cluster around estuaries for food, transportation and other needs invariably results in construction on the flood plains. The result has often been periodic flooding problems at times of major flood events. Numerical models offer potential for improved environmental impact assessment of construction on estuarine flood plains.

Over the past ten to fifteen years, numerical modelling of hydrodynamic systems has become an established science. A variety of numerical models are available based on both finite difference and finite element formulations of the basic governing equations. Hydrodynamic systems are basically three-dimensional; however, for many situations conditions are such that the flow can be satisfactorily approximated by a simplified set of governing equations. The two dimensional depth averaged model has been shown by a number of investigators (3, 4, 7, 10, 11) to satisfactorily represent flow in an estuary or bay when the water body is not stratified.

1. Professor of Engineering Mechanics, The University of Alabama, Tuscaloosa, AL
2. Professor of Mechanical Engineering, The University of Alabama, Tuscaloosa, AL
3. Graduate Research Assistant, The University of Alabama, Tuscaloosa, AL

The present contribution presents a specific application of a two-dimensional depth average finite difference numerical model for flood plain investigations. Flooding problems which exists on Bayou Sara, a bayou on the flood plains above Mobile Bay, are considered. A railroad constructed on a fill crosses the flood plains with trestles at major streams. Because of the location of Bayou Sara relative to the railroad, some speculation exists concerning the effect which the railroad has upon flooding problems which are encountered along the bayou. The numerical model is used to investigate the influence which the railroad exerts on flood stages along Bayou Sara. The model is partially calibrated and verified using available prototype data for known flood events. Boundary conditions are used which produce a range of possible flood events. The two year, five year, ten year, twenty-five year, fifty year, one hundred year and five hundred year probability flood events are of particular interest. For each flood event the model was applied for existing conditions and also the condition without the railroad on the flood plains. Differences between flow patterns, flow rates and flood stage elevations are documented. From these differences an assessment can be made of the railroad influence on flooding along Bayou Sara.

The numerical model has general applicability to similar flooding problems on estuarine flood plains. Availability of accurate model input data and flood stage water elevations for model calibration and verification is generally the limiting factor on the accuracy of results.

THE NUMERICAL MODEL

A complete mathematical description of the hydrodynamic flow in a harbor, bay or estuary would require that the velocity and density be

completely specified for every point in the system at all times:

$$u = u\,(x,y,z,t)$$

$$\rho = \rho\,(x,y,z,t)$$

where

x = longitudinal coordinate measured along the estuary axis

y = transverse coordinate

z = vertical coordinate

t = time

Because of the difficulties in formulating, executing and verifying a three-dimensional model, researchers have devised a variety of numerical models of various degrees of simplification.

A two-dimensional depth averaged model (BAY) is used in this investigation. The vertical components of velocity and acceleration are neglected and the general three-dimensional governing hydrodynamic equations are integrated over the water depth. A pseudo-three-dimensional effect is present since the equations are forced to satisfy the boundary conditions at the bottom and surface of the water column. A depth-averaged two-dimensional flow field is obtained but three-dimensional geometry can be considered. The most important approximations used in the model are those of constant density and relatively small variations of velocity over the depth, conditions which should be reasonably valid in the Mobile Bay delta. Where these conditions are approximately valid, this type of numerical model can provide accurate representations of tidal elevations and velocities.

The rectangular coordinate system is located in the plane of the undisturbed water surface as shown in Figure 1. The equations of motion

and the equation of continuity are written as follows:

$$\frac{\partial u}{\partial t} + u\frac{\partial u}{\partial x} + v\frac{\partial u}{\partial y} + g\frac{\partial \eta}{\partial x} - fv = R_x + L_x \tag{1}$$

$$\frac{\partial v}{\partial t} + u\frac{\partial v}{\partial x} + v\frac{\partial v}{\partial y} + g\frac{\partial \eta}{\partial y} + fu = R_y + L_y \tag{2}$$

and

$$\frac{\partial \eta}{\partial t} + \frac{\partial}{\partial x}\left[(h+\eta)u\right] + \frac{\partial}{\partial y}\left[(h+\eta)v\right] = 0 \tag{3}$$

where

u = depth-averaged velocity comoponent in the x-direction

t = time

x,y = rectangular coordinate variables

v = depth-averaged velocity component in the y-direction

g = acceleration due to gravity

η = water level displacement with respect to datum elevation

f = Coriolis parameter

R_x, R_y = the effect of bottom roughness in x and y directions

L_x, L_y = the effect of the wind stress acting on the water surface in the x and y directions

h = water depth

The continuity equation has been obtained by integrating across the water depth and applying kinematic and dynamic boundary conditions at the surface and bottom of the reservoir. The bottom friction terms are represented by:

$$R_x = \frac{-gu(u^2+v^2)^{\frac{1}{2}}}{C^2(h+\eta)} \tag{4}$$

$$R_y = \frac{-gv(u^2+v^2)^{\frac{1}{2}}}{C\ (h+\eta)} \tag{5}$$

where C is the Chezy coefficient. The wind stress terms are of the form:

$$L_x = \frac{T_x}{(h+\eta)} \tag{6}$$

$$L_y = \frac{T_y}{(h+\eta)} \tag{7}$$

where T_x and T_y are the wind stress components acting on the water surface.

A major advantage of BAY is the capability of applying a smoothly varying grid to the given study region. This allows efficient simulation of complex geometries by locally increasing grid resolution in critical areas. For each coordinate direction, a piecewise reversible transformation is independently used to map prototype or real space (x,y space) into a computation space (α_1, α_2 space). The transformation takes the form

$$x = a + b\alpha^c \tag{8}$$

where a, b and c are arbitrary constants. By applying a smoothly varying grid transformation which is continuous and which has continuous first derivatives, many stability problems commonly associated with variable grid schemes are eliminated provided that all derivatives are centered in space (17). The transformed equations in space can be written as

$$\frac{\partial u}{\partial t} + \frac{1}{\mu_1} u \frac{\partial u}{\partial \alpha_1} + \frac{1}{\mu_2} v \frac{\partial u}{\partial \alpha_2} + \frac{g}{\mu_1} \frac{\partial \eta}{\partial \alpha_1} - fv = R_x + L_x \tag{9}$$

$$\frac{\partial v}{\partial t} + \frac{1}{\mu_1} u \frac{\partial v}{\partial \alpha_1} + \frac{1}{\mu_2} v \frac{\partial v}{\partial \alpha_2} + \frac{g}{\mu_2} \frac{\partial \eta}{\partial \alpha_2} + fu = R_y + L_y \tag{10}$$

$$\frac{\partial \eta}{\partial t} + \frac{1}{\mu_1} \frac{\partial}{\partial \alpha_1} [(h+\eta)u] + \frac{1}{\mu_2} \frac{\partial}{\partial \alpha_2} [(h+\eta)v] = 0 \tag{11}$$

To solve the governing equations, a finite difference approximation

of the equations and an alternating direction technique are employed. The solution scheme is similar to that proposed by Leendertse (6). A space-staggered scheme is used in which velocities, water-level displacement, bottom displacement, and water depth are described at different locations within a grid cell as shown in Figure 2. Central differences are used for evaluating all derivatives in the governing equations. The application of these difference approximations gives rise to corresponding difference equations centered about different points within a grid cell. These expressions require the evaluation of certain quantities at locations different from those defined in the grid system. Such quantities are replaced by values computed from one- and two-dimensional averaging of neighboring values.

Three types of boundaries are involved in the calculations: solid boundaries at fixed coastlines, artificial tidal input boundaries arising from the need to truncate the region of computation and river inflows into the bay.

The boundary condition for the solid boundary can be written as

$$\vec{V} = 0 \tag{12}$$

where $\vec{V}_n$ denotes the normal component of velocity. Artificial tidal boundaries were used in the model to describe the tidal action that occurs at the bay computational boundaries. The water surface elevation-time history for the desired tidal cycle is specified at each such boundary and applied during the operation of the model. River inflow boundaries are required to simulate the river hydrograph for these significant streams discharging into the study region.

MOBILE BAY DELTA SYSTEM

Mobile Bay is the terminus of the fourth largest river system, in terms of discharge, in the contiguous United States (8) and the sixth largest on the North American Continent (5). The river system discharging into Mobile Bay is a complex one as is illustrated in Figure 3. In simplified form, the river system can be considered to start at the confluence of the Alabama and Tombigbee Rivers where the Mobile River is formed. The Mobile River then divides into the Tensaw and lower Mobile Rivers. Both of these rivers branch many times producing a complex network of major channels, creeks, and bayous. The river system flows over a flood plain which extends for over 30 miles south terminating at the northern end of Mobile Bay.

The average discharge of the river system (1929-1978) into the bay is approximately 64,100 cfs (1815m^3/sec) (10). The monthly average discharges have a high flow in February, March and April and a low flow period between June and November.

Significant flooding is considered to occur when flows exceed approximately 247,000 cfs (6994m^3/sec) (13). A table of probability floods is shown in Table 1. At the delta-bay interface the lower Mobile River and three distributaries, the Tensaw-Spanish River, the Apalachee River and the Blakeley River discharge into Mobile Bay. At the upper end of the study area, I-65 cuts across several water bodies, the Mobile River, Little Lizard Creek, Mifflin Lake, the Middle River, and the Tensaw River. Between the boundaries for the study area lies a great deal of flood plains with an elevation only a few feet above mean sea level. During flood conditions great deal of water is stored on these flood plains. There have been several general studies (12, 14, 15) of the marsh

flood plain areas and the effects of river flooding in Mobile Bay. Little attention, however, has been focused on flooding problems in the delta region.

The railroad generally follows a northeast to southwest path across the delta which basically has a north-south alignment. As indicated in Figure 3, Bayou Sara is located in the west-central region of the delta. The geometry of the system suggests that the railroad might have an effect on flood stage elevations along Bayou Sara.

THE FINITE DIFFERENCE GRID

The finite difference grid, Figure 4, used to model of Mobile Bay delta system was developed using a 1:24000 scale nautical chart (16). A variable grid was developed with the primary objective of good resolution of the main river channels and the area around Bayou Sara. A reasonable representation of other geometric and bathymetric features of the area was established. The dimension of the resulting grid was 78 by 38 cells or 2964 cells. After mapping the grid, it was used as an overlay on the nautical chart to assign boundaries, depth and Manning friction coefficients for each finite difference cell. A set of aerial photographs (11) of the delta region taken during February 1982 was also useful in developing the finite difference grid and other input data for the numerical model. Information on construction details of the railroad across the flood plains was also used in establishing the finite difference grid. The manner in which the grid represents the major channels in the study area is illustrated in Figure 5.

The smallest cells were used in representing the area around Bayou Sara since this was the region of primary interest. Small cells were also

used for the major river channels. Larger cells were used on the flood plain areas where the bathymetry was reasonably constant and/or boundary geometry was relatively simple. The smallest cell size was 500 feet and the maximum depth was approximately 45 feet.

Elevation boundary conditions were specified at the Mobile Bay boundary and upstream at the I-65 boundary. The Mobile Bay elevation is primarily dominated by the tide while the elevation boundary condition specified at I-65 is representative of the flood stage. An elevation boundary condition was applied at I-65 rather than a flow boundary condition because of greater accuracy in imposing the boundary condition in the numerical model.

Depths were assigned to each water cell as delineated by the land boundary. The depth of each cell was determined as a weighted average of the charted depths within that cell. Because of a lack of bathymetric and topographic data for the flood plains, most of these areas were considered to have the same elevation. In areas where the finite difference cell is larger than the actual physical dimension, cell depths were reduced in the model to make the flow cross-sectional areas approximately equal. Manning's n friction values for bottom roughness were assigned on a relative basis according to the bottom type specified by the nautical chart.

The datum of the nautical chart was the National Geodetic Vertical Datum of 1929 (N.G.V.D.). All elevations used in the study were established relative to this datum. Most of the flood plains are only slightly above the N.G.V.D. reference in elevation and are flooded during the flood events to be simulated.

MODEL CALIBRATION AND VERIFICATION

A numerical model must be calibrated and verified before a great deal of confidence is placed in the model results. Calibration consists of demonstrating that the numerical model can be adjusted to produce results which are consistent with a measured prototype data set. Verification consists of applying the calibrated model and reproducing a second set of prototype data to a reasonable degree of accuracy.

For this study one relatively complete set of prototype data (9) was available representing high water elevations around the delta region for the flood event of March 1979. This data set was used to calibrate the model. A partial data set (9) of high water elevations was available for the Spring 1979 flood event. These data were used to provide a limited verification of the numerical model.

The measured high water elevations at I-65 provided a basis for establishing the northern elevation boundary conditions for model calibration. The tidal elevations measured in Mobile Bay provided the boundary condition for the southern boundary of the model. The model was started with a constant water elevation throughout the delta region including the flood plains. The boundary conditions were then allowed to gradually change until the desired flood condition was reached in about 18 hours. The boundary conditions were then held constant for approximately 6 hours so that a quasi-steady state condition was reached in the model. For a more detailed study actual river hydrographs should be used as the river boundary condition. Flood stage elevations at 13 locations in the delta region and the system flow rate were the primary variables used in establishing model calibration and verification. The special gage point

locations are shown in Figure 6.

The calibration and verification process was continued until agreement was reached between the numerical model and the prototype data sets. A vector plot of the flow pattern for the calibration run is shown in Figure 6. Observe that most of the flow follows the channel with only small velocities on the flood plain areas. Additional results from the calibration and verification process are shown in the next section of the paper along with other model results. An average height of 1.9 feet above N.G.V.D. for the flood plains appeared to produce the most satisfactory results. Manning n values between 0.021 and 0.07 were used.

MODEL APPLICATIONS AND RESULTS

The numerical model was applied for a range of upstream elevation boundary conditions. The lower boundary condition, dominated by the bay tide, was maintained as that used for model calibration. Different upstream boundary elevations were selected to produce flood events with a range of flow rates between approximately 200,000 cfs (5660 m^3/sec) and 800,000 cfs (22,700 m^3/sec). This range of flow rates contains the 2 year, 5 year, 25 year, 50 year, 100 year and 500 year probability flood events. In each case, the starting condition for the model was an initial constant water elevation and zero velocity in the delta region. The boundary conditions were then allowed to change to produce the desired quasi-steady state flood event in approximately 24 hours. For each set of boundary conditions there were two model applications. The first model application was for existing conditions; i.e., with the railroad crossing the flood plains. The railroad fill was then replaced by flood plains

with friction and depth characteristics similar to surrounding areas.

Figure 7 illustrates the calculated flood stage elevations at one of the special gage points in the delta system as a function of flow rate. Results for existing conditions and for the without railroad case are presented in the figure along with prototype data used for calibration and verification. The numerical model was found to be in general agreement with prototype data for the entire delta region. The railroad does not appear to produce large changes in flood elevations at any of the points in the delta region where prototype data were available. The largest effects at any of the special gage points are in the Bayou Sara area, but even here effects are small compared with the overall flood stage elevation.

Sample vector plots of overall flow patterns in the delta region are presented in Figures 8 and 9. Figure 8 is for existing conditions while Figure 9 represents the flow pattern if the railroad did not cross the flood plains. These plots clearly indicate that most of the flow passes along the existing channels regardless of whether the railroad exists or does not exist on the flood plains. There is a great deal of water stored on the flood plains, but there is not a large quantity of flow along (north to south) or across (east to west) the flood plains. The large friction and small depth conditions on the flood plains are not conducive to large flows.

Representative contour plots of flood stage elevation in the delta region are presented in Figures 10 and 11. Figure 10 is for the existing condition and Figure 11 is for the case without the railroad on the flood plains. These contour plots indicate that the railroad does produce significant differences in flood stage elevations within the interior of

the delta region; there is almost 2 ft (0.61 m) differences in elevation across the railroad fill in some locations. Figure 12 represents a contour plot for the difference in flood stage elevation which can be attributed to the railroad crossing the flood plains. Some large differences are observed in the interior of the delta but only relatively small differences extend to the boundary areas.

CONCLUSIONS

The numerical model was calibrated and verified to an extent consistent with the objectives of this investigation. The flows in the delta region are found to be primarily within the existing channels with only a relatively small percentage of the flows along or across the flood plains. Significant differences in flood stage elevations are produced by the railroad within some interior regions of the delta; i.e., across the railroad fill. However, these regions where significant effects are observed are confined to restricted regions within the interior of the delta. The effects are relatively small around the boundaries of the delta.

Based upon the numerical model results, the increase in flood stage elevation along Bayou Sara is small compared with the overall flood stage elevation. Below a system flow rate of 200,000 cfs (5,660 m^3/sec) there is a negligible effect caused by the railroad. On a statistical basis, a 200,000 cfs (5,660 m^3/sec) flow rate corresponds to a flood event which should occur once each year. The railroad effect at Bayou Sara increases up to approximately six to eight inches (15.2 to 20.3 cm) for a flow rate of 700,000 cfs (19,800 m^3/sec). A 700,000 cfs (19,800 m^3/sec) flow rate corresponds to a flood event which has a 500 year statistical rate of

occurrence. The effects of the railroad on flood stage elevations along Bayou Sara is therefore small compared with overall flood stage elevations.

ACKNOWLEDGEMENT

This study was sponsored by the U.S. Corps of Engineers, Mobile District. The authors are grateful to the agency and the individuals who made this study possible. Tim Phillips and Maurice James of the U.S. Corps of Engineers, Mobile District Office, provided valuable assistance as well as providing the necessary prototype data for calibration and verification of the model.

TABLE I

FLOW RATE - EXPECTED PROBABILITY DATA FOR MOBILE RIVER AT BARRY STEAM PLANT (BUCKS, ALABAMA)

STATISTICAL RATE OF OCCURRENCE (YRS)	EXPECTED FLOW RATE (CFS)
2	284,000 (8,040 m^3/sec)
5	371,000 (10,500 m^3/sec)
10	425,000 (12,000 m^3/sec)
25	491,000 (13,900 m^3/sec)
50	540,000 (15,300 m^3/sec)
100	588,000 (16,700 m^3/sec)
500	700,000 (19,800 m^3/sec)

APPENDIX I - REFERENCES

1. Aerial Survey Photographs by Continental Aerial Surveys under contract to U.S. Army Corps of Engineers, Mobile District, February 22-26, 1982.

2. Bault, E.I., "Hydrology of Alabama Estuarine Areas - Cooperative Gulf of Mexico Estuarine Inventory", Alabama Marine Res. Bulletin 7, pp. 1-36, 1972.

3. Butler, H.L. and Raney, D.C., "Finite Difference Schemes for Simulating Flow in an Inlet-Wetlands Sytstem", Proceedings, 1976, Army Numerical Analysis and Computers Conference, Report 76-3, pp. 471-508, Army Research Office, Research Triangle Park, NC, September 1976.

4. Butler, H.L., "Evaluation of a Numerical Model for Simulating Long-Period Wave Behavior in Ocean-Estuarine Systems", Estuarine and Wetland Processes with Emphasis on Modeling, Marine Science Series, Vol. II, Plemen Press, New York, 1980.

5. Chow, V.T., Handbook of Applied Hydrology, McGraw-Hill, New York, 1968.

6. Leendertse, J.J., "Aspects of Computational Model for Long-Period Water-Wave Propagation", RM-5294-PR, Rand Corporation, Santa Monica, CA, 1967.

7. Leendertse, J.J., "A Water-Quality Simulation Model for Well-Mixed Estuaries and Coastal Seas, Vol. I, Principles of Computation, RM-6230-RC, Rand Corporation, Santa Monica, CA, February, 1970.

8. Morisawa, M., "Streams, Their Dynamics and Morphology, McGraw-Hill, New York, 1968.

9. Package of data on floods and L&N Railroad provided by U.S. Army Corps of Engineers, Mobile District.

10. Raney, D.C. and Butler, H.L., "Landslide Generated Water Wave Problem", Journal of Hydraulic Division, ASCE, Vol. 102, No. HY9, Proc. Paper 12425, pp. 1269-1282, September 1976.

11. Reid, R.O. and Bodine, B.R., "Numerical Model for Storm Surges in Galveston Bay", Journal of Waterways and Harbors Division, ASCE, Vol. 94, No. WW1, February 1968, Proc. Paper, 5805, pp. 33-57.

12. Schroeder, W.W., "The Impact of the 1973 Flooding of the Mobile River System on the Hydrography of Mobile Bay and East Mississippi Sound", Northeast Gulf Science, Vol. 1, No. 2, pp. 68-75, December 1977.

13. Schroeder, W.W., Riverine Influence on Estuaries: A Case Study, in M.S. Wiley (ed.), Estuarine Interactions, Academic Press, Inc., New York, 1978, pp. 347--364.

APPENDIX I - REFERENCES (continued)

14. Schroeder, W.W., "Dispersion and Impact of Mobile River System Waters in Mobile Bay, Alabama", Water Resources Research Institute Bulletin 37, Auburn University, August 1979.

15. Stout, Judy P., "Marshes of the Mobile Bay Estuary: Status and Evaluation", Symposium on the Natural Resources of the Mobile Estuary, Alabama, pp. 113-122, May 1979.

16. U.S. Geological Survey 7.5 Minute Topographic Maps, 1:24,000 scale (Bridgehead, Chickasaw, Hurricane, Mobile, Bay Minnette North and the basic of quadrangles).

17. Wanstrath, J.J., Whitaker, R.E., Reid, R.O. and Vastand, A.C., "Storm Surge Simulation in Transformed Coordinates, Vol. I - Theory and Application", Technical Report 76-3, U.S. Army Coastal Engineering Research Center, CE, Fort Belvoir, VA, November, 1976.

LIST OF FIGURES

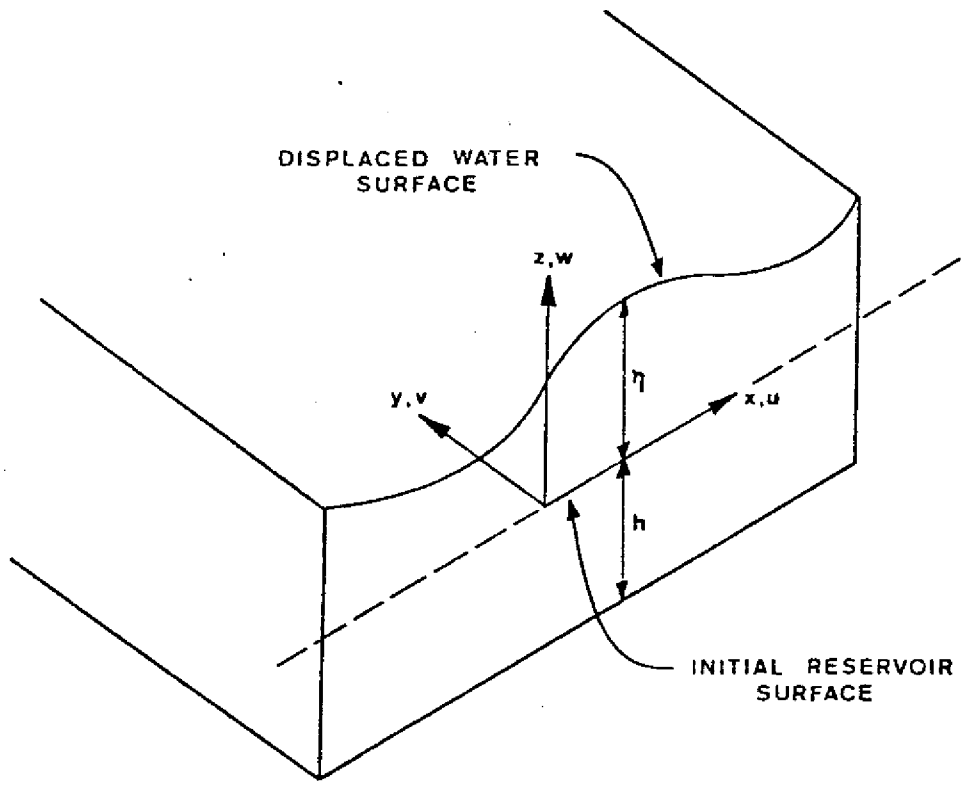

Figure 1. Coordinate System for Problem Formulation

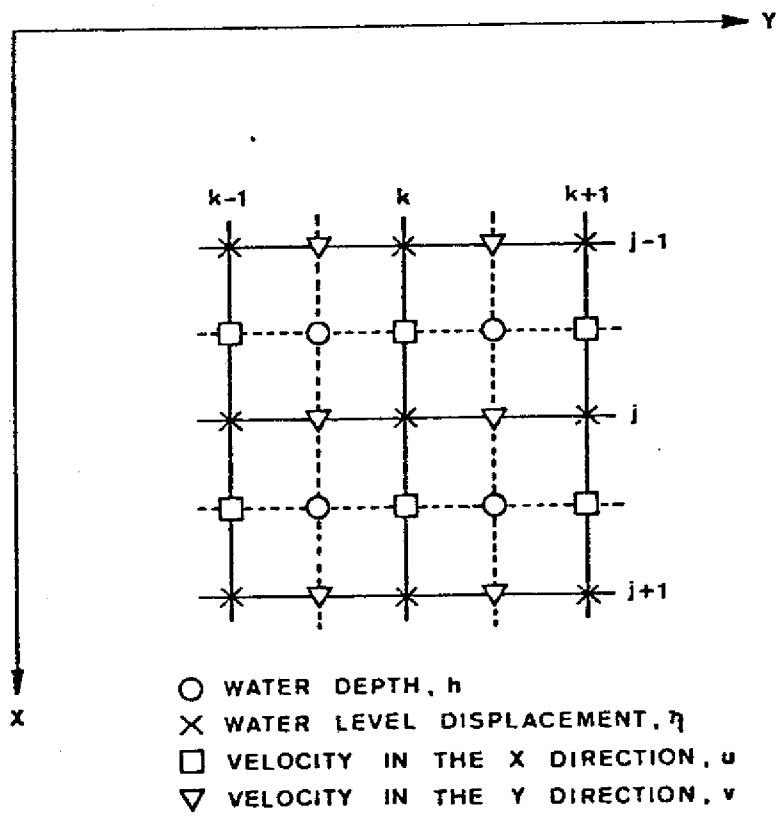

Figure 2. Grid System and Variable Definition Locations

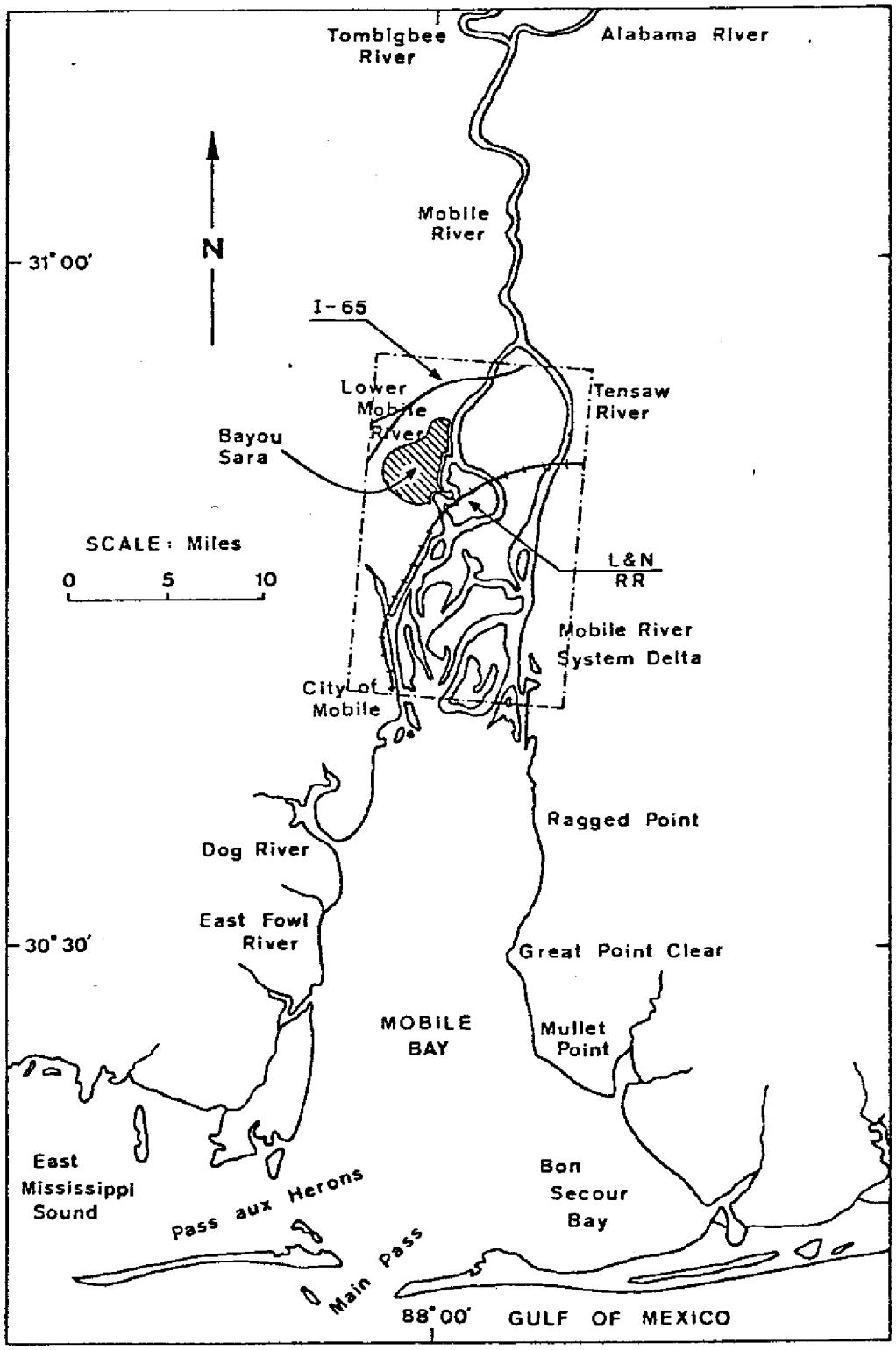

Figure 3. Mobile Bay and River Delta System

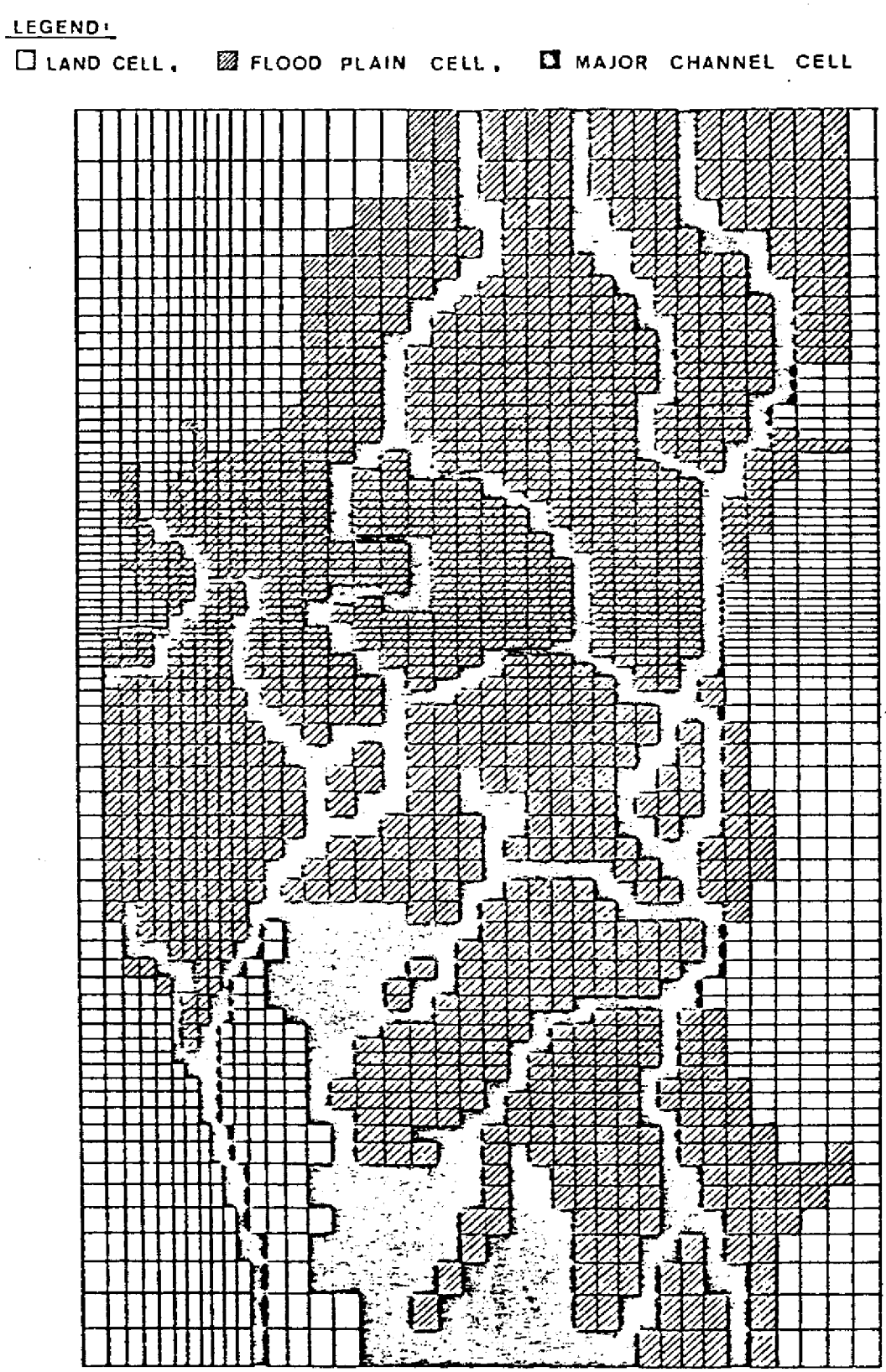

Figure 4. The Variable Size Finite Difference Grid

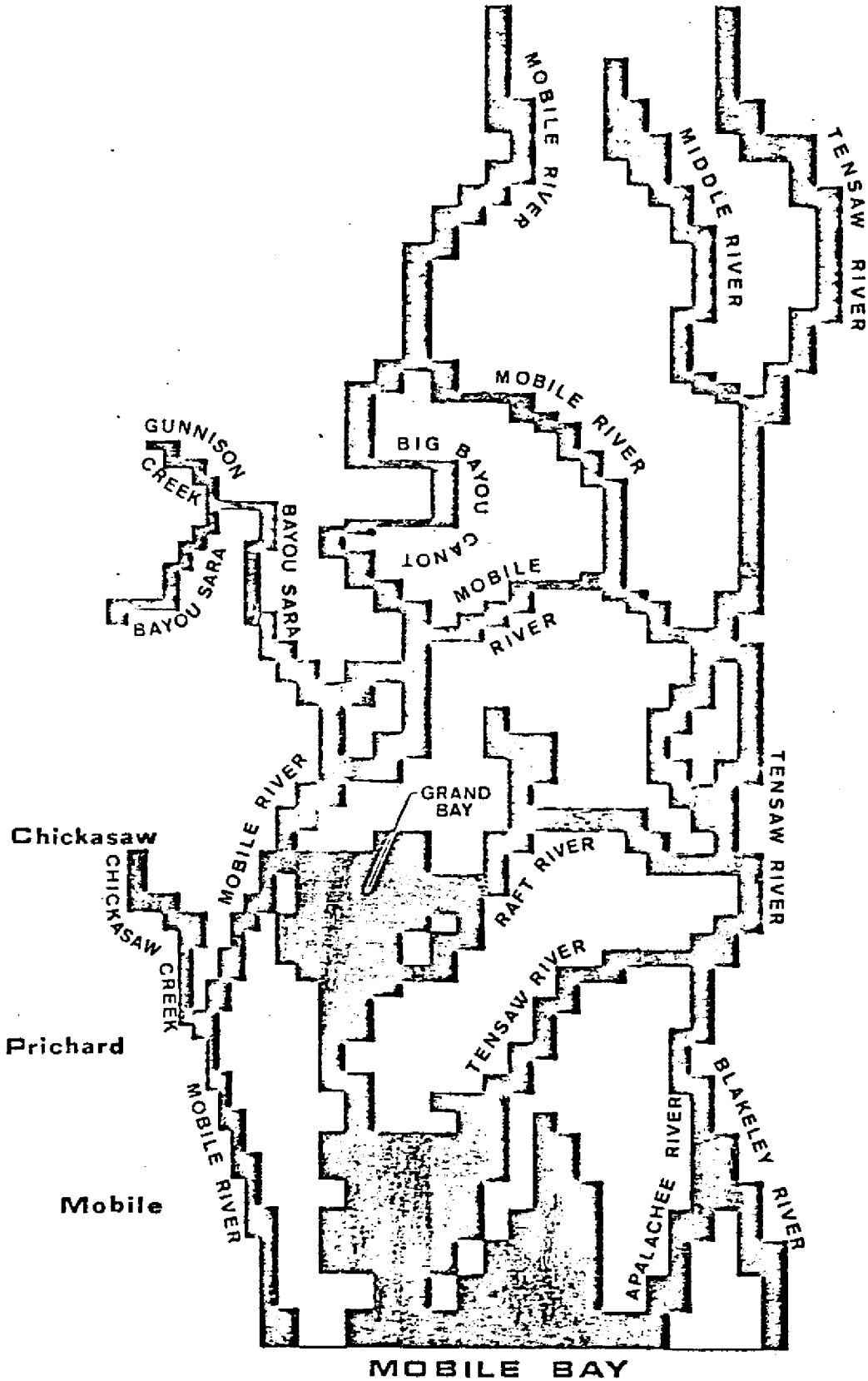

Figure 5. Representation of Major Channels by the Finite Difference Grid

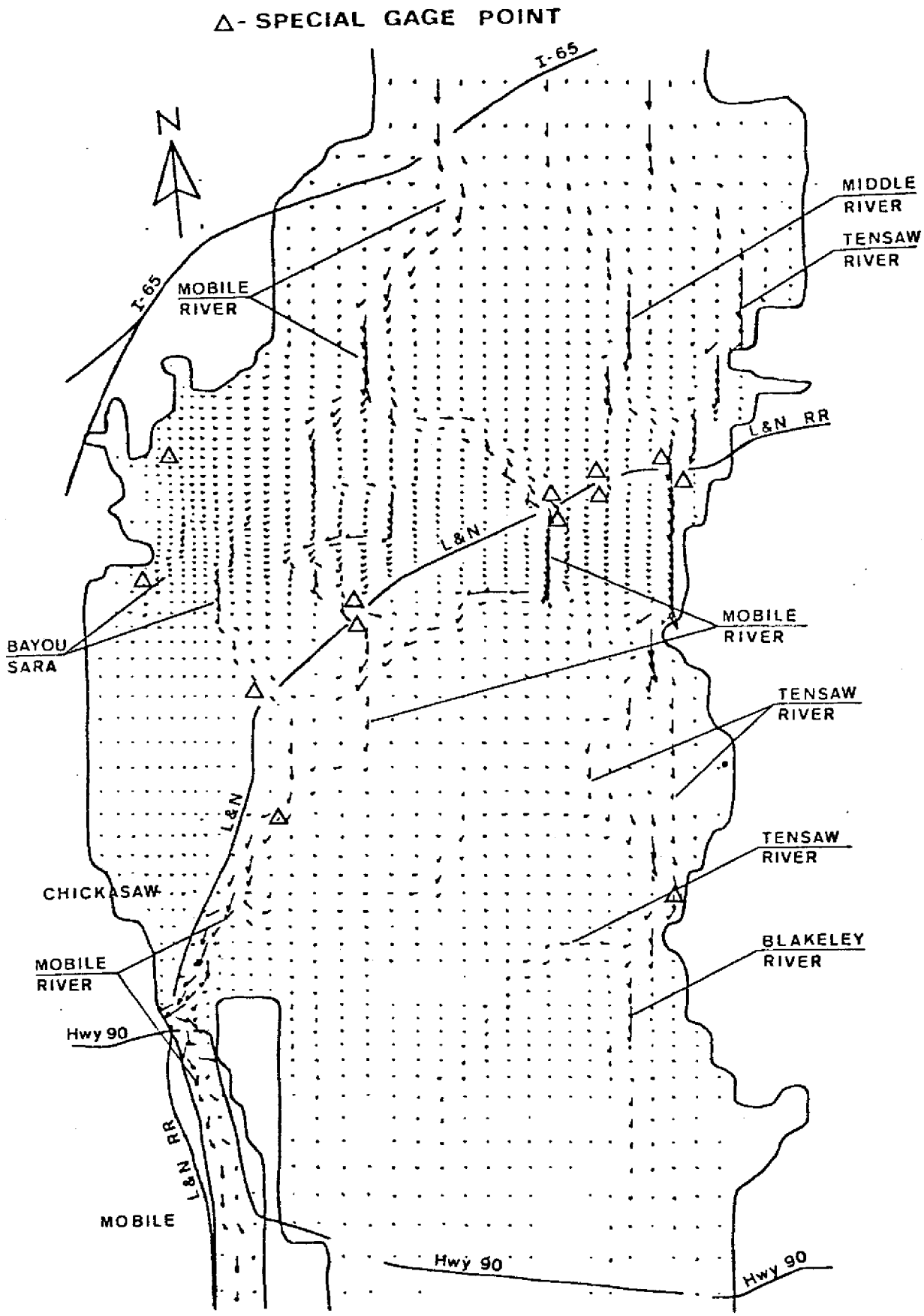

Figure 6. Vector Plot of Velocity Pattern in Delta Region for Calibration Condition

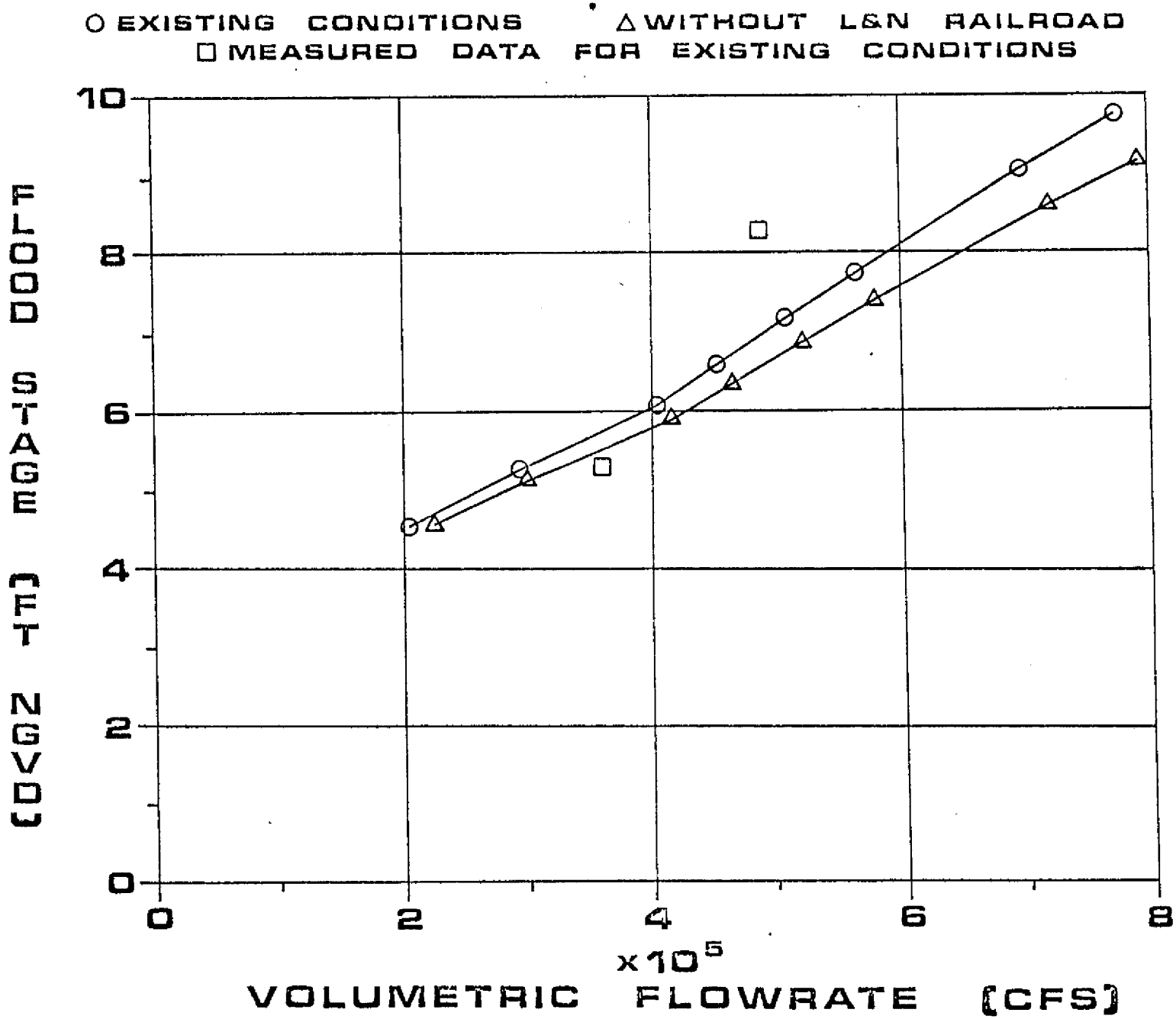

Figure 7. Flood Stage (N.G.V.D.) on Bayou Sara (near Satsuma) as a Function of Flow Rate

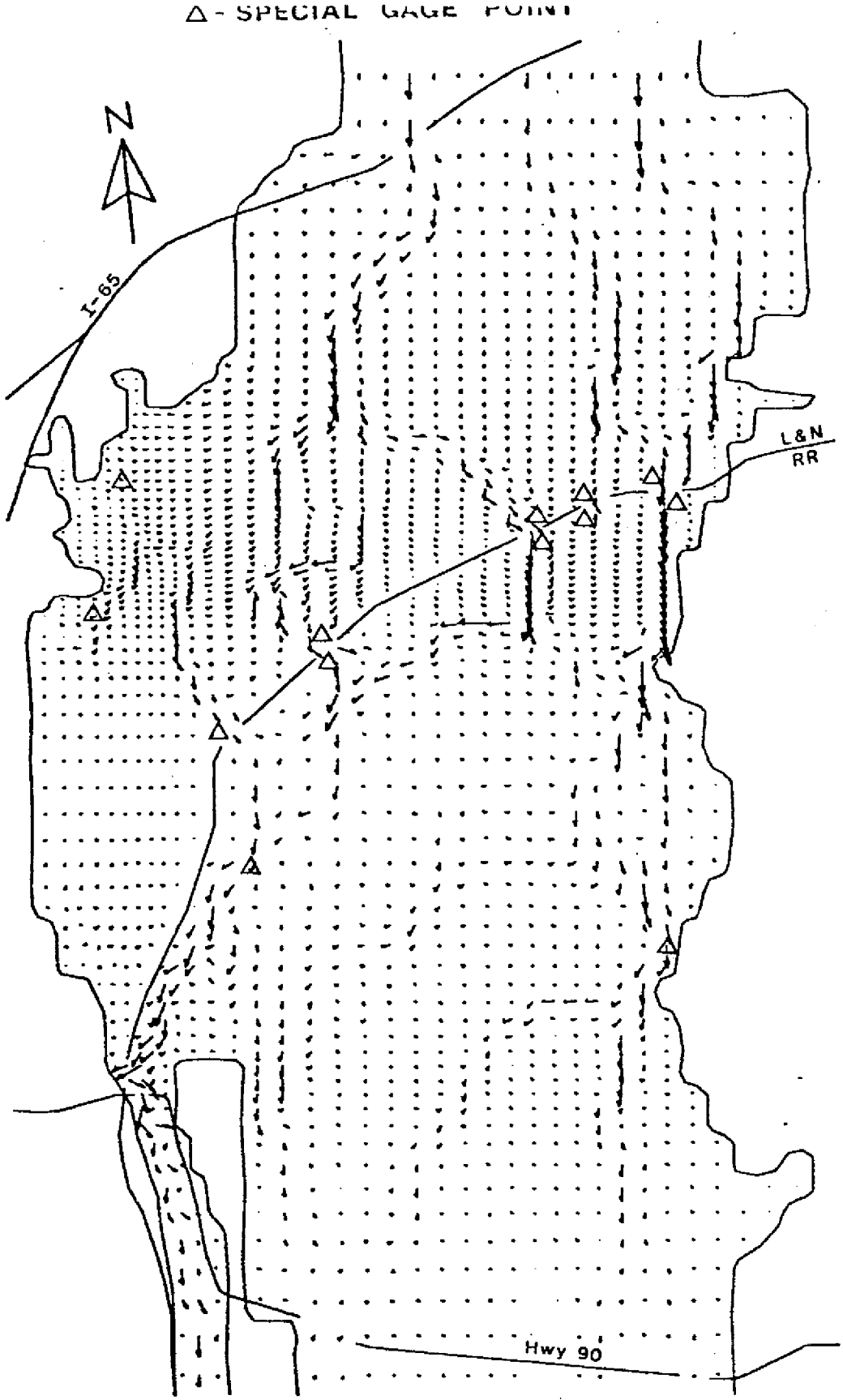

Figure 8. Overall Flow Patterns in the Mobile Bay Delta Region for a Flow Rate of 504,327

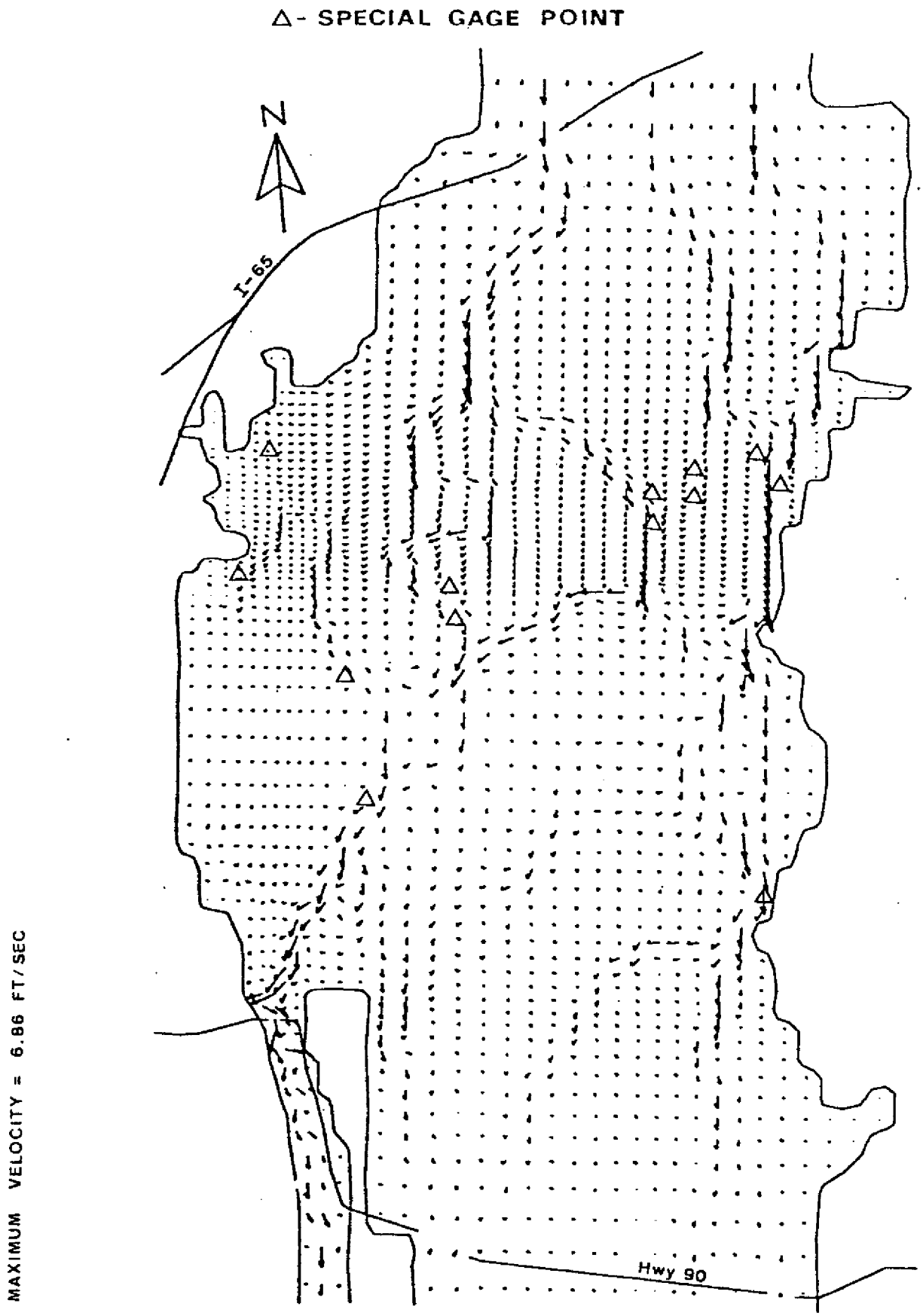

Figure 9. Overall Flow Patterns in the Mobile Bay Delta Region (without the L&N Railroad) for a Flow Rate of 518,636 cfs

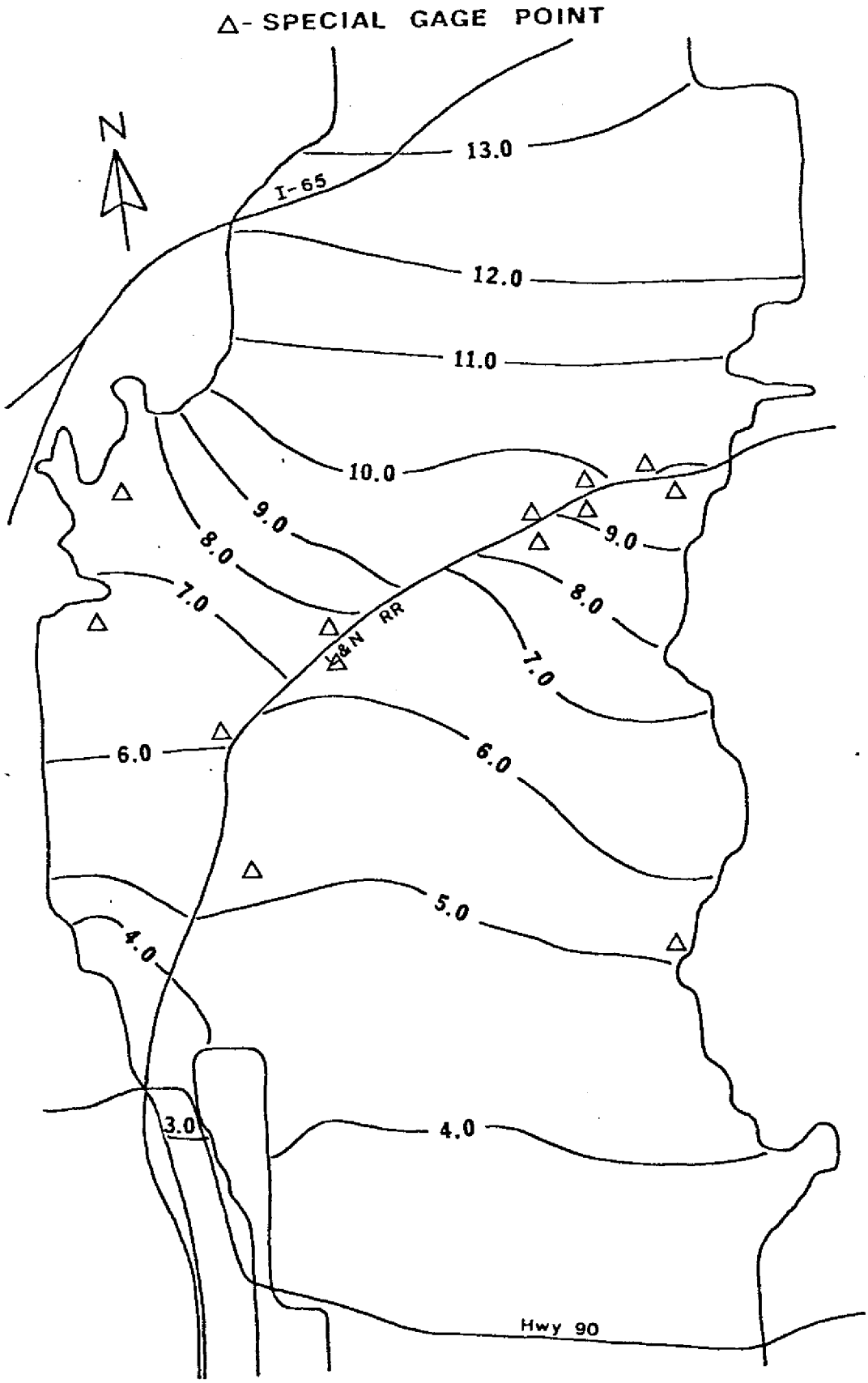

Figure 10. Flood Stage Contours (in feet) in the Mobile Bay Delta Region for a Flow Rate of 504,327 cfs.
(1 ft = 0.305m, 1 cfs = 0.028 m^3/sec)

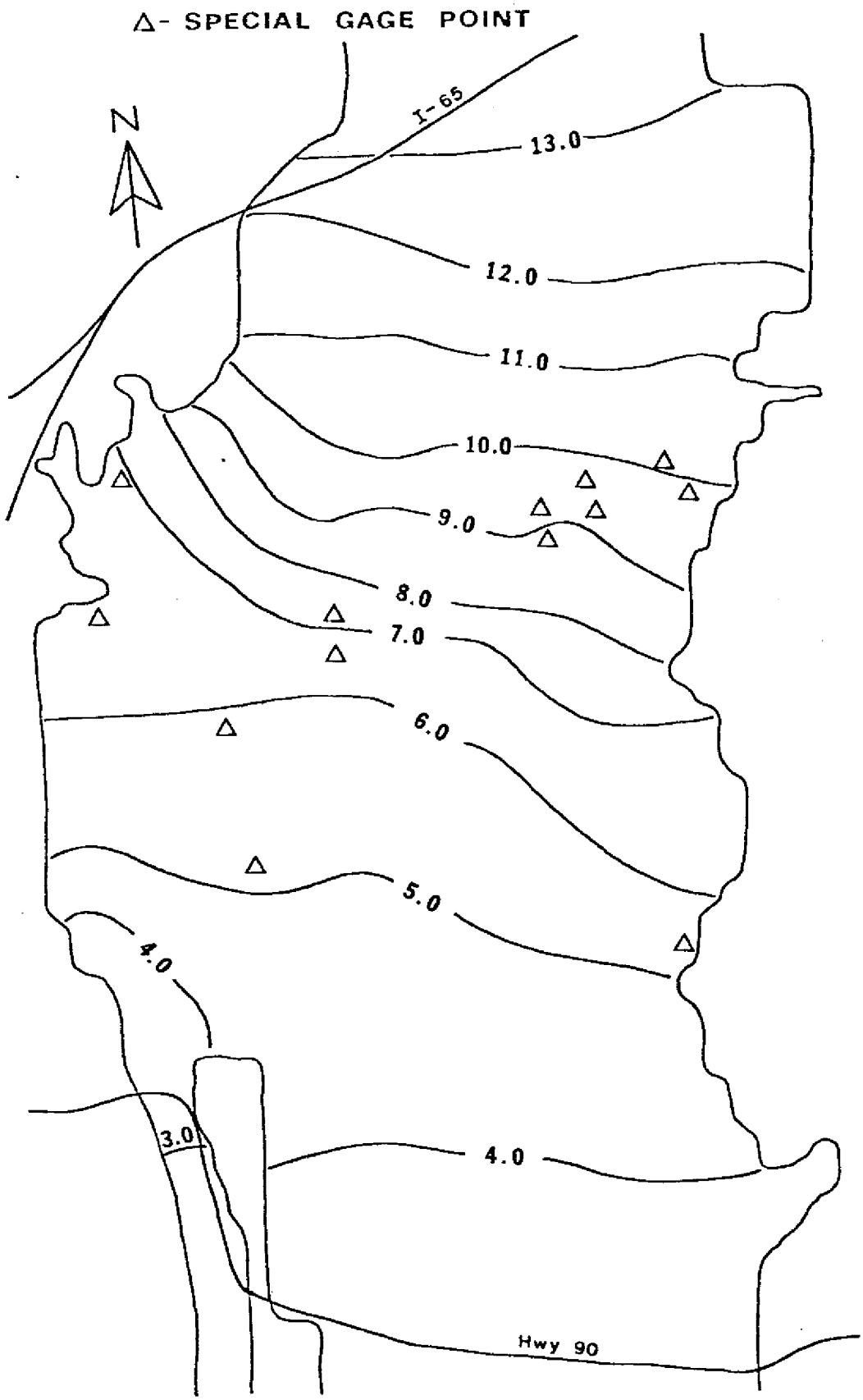

Figure 11. Flood Stage Contours (in feet) in the Mobile Bay Delta Region (without the L&N Railroad) for a Flow Rate of 518,636 cfs. (1 ft = 0.305m, 1 cfs = 0.028 m^3/sec)

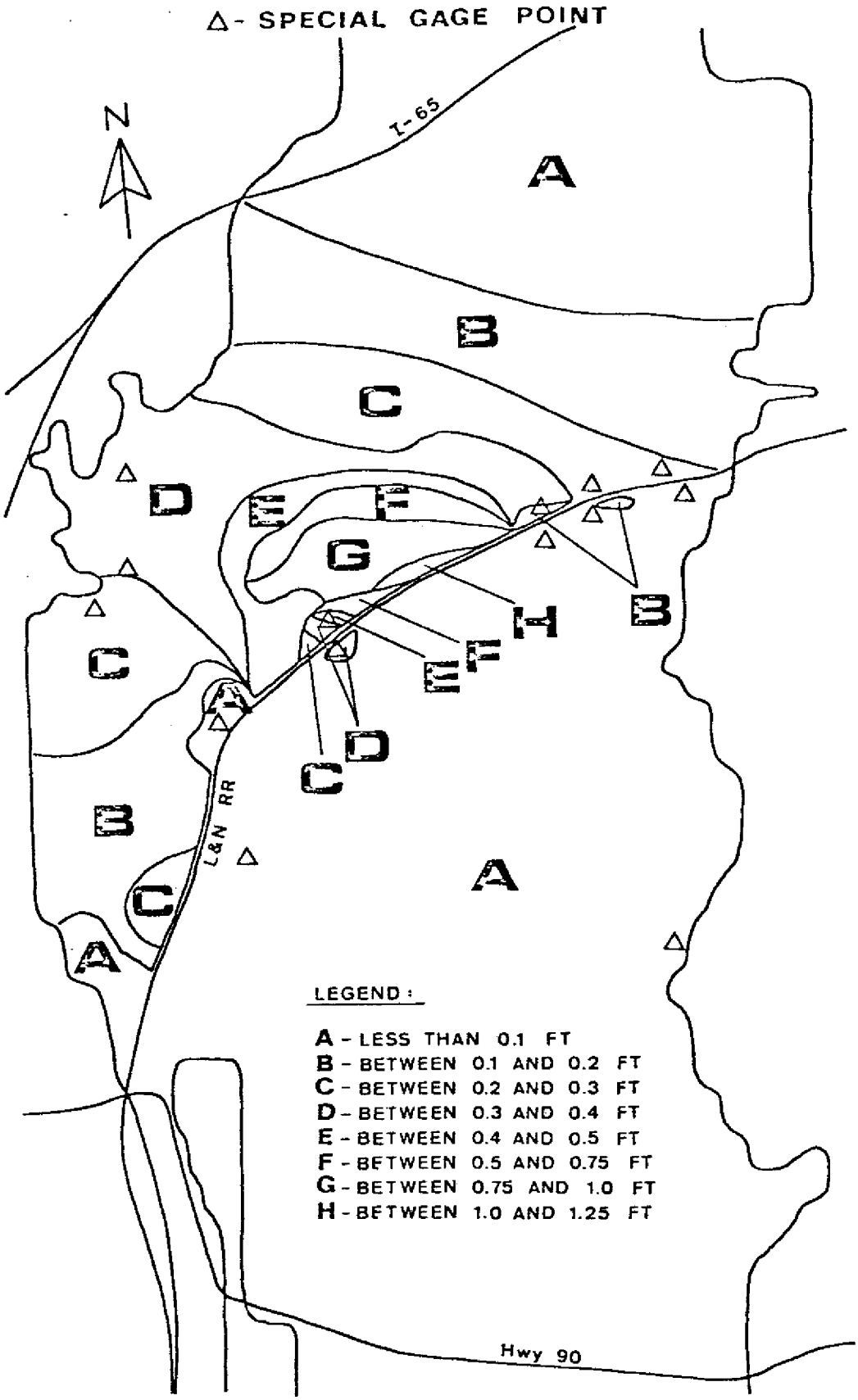

Figure 12. Differences in Flood Stage Elevations in the Mobile Bay Delta Region as a Result of the L&N Railroad for a Flow Rate of Approximately 510,000 cfs.
(1 ft = 0.305m, 1 cfs = 0.028 m^3/sec)